

LEGIBILITY NOTICE

A major purpose of the Technical Information Center is to provide the broadest dissemination possible of information contained in DOE's Research and Development Reports to business, industry, the academic community, and federal, state and local governments.

Although a small portion of this report is not reproducible, it is being made available to expedite the availability of information on the research discussed herein.

5/12/88 8:52 (5)

DR# 0588-6

ORNL-6472

ornl

**OAK RIDGE
NATIONAL
LABORATORY**

MARTIN MARIETTA

Development of Ferritic Steels for Fusion Reactor Applications

R. L. Klueh
P. J. Maziasz
W. R. Corwin

OPERATED BY
MARTIN MARIETTA ENERGY SYSTEMS, INC
FOR THE UNITED STATES
DEPARTMENT OF ENERGY

DISTRIBUTION OF THIS DOCUMENT IS UNLIMITED

Printed in the United States of America Available from
National Technical Information Service
U S Department of Commerce
5285 Port Royal Road, Springfield, Virginia 22161
NTIS price codes -Printed Copy A05 Microfiche A01

This report was prepared as an account of work sponsored by an agency of the United States Government. Neither the United States Government nor any of its employees makes any warranty, express or implied, or assumes any legal liability or responsibility for the accuracy, completeness, or usefulness of any information, apparatus, product, process, or service disclosed, or represents that its use would not infringe privately owned rights. Reference herein to any specific commercial product process, or service by trade name, trademark, manufacturer, or otherwise, does not necessarily constitute an endorsement, recommendation, or favoring by the United States Government or any agency thereof. The views and conclusions contained herein are not necessarily those of the United States Government or any agency thereof.

ORNL-6472
Distribution
Category UC-423

Metals and Ceramics Division

DEVELOPMENT OF FERRITIC STEELS FOR FUSION REACTOR APPLICATIONS

R. L. Klueh
P. J. Maziasz
W. R. Corwin

ORNL--6472

DE89 001141

Date Published - August 1988

Prepared for
DOE Office of Fusion Energy
AT 15 02 03 A

Prepared by the
OAK RIDGE NATIONAL LABORATORY
Oak Ridge, Tennessee 37831
operated by
MARTIN MARIETTA ENERGY SYSTEMS, INC.
for the
U.S. DEPARTMENT OF ENERGY
under Contract DE-AC05-84OR21400

MASTER

Sc

DISTRIBUTION OF THIS DOCUMENT IS UNLIMITED

CONTENT

LIST OF FIGURES	v
LIST OF TABLES	ix
ABSTRACT	1
INTRODUCTION	2
EXPERIMENTAL PROCEDURE	5
RESULTS	9
OPTICAL MICROSCOPY	9
TRANSMISSION ELECTRON MICROSCOPY	12
PRECIPITATE IDENTIFICATION	27
HEAT TREATMENT STUDIES	32
Austenitizing Behavior	32
Tempering Behavior	32
ELIMINATION OF DELTA-FERRITE FROM 12Cr-2WV STEEL	39
TENSILE PROPERTIES	41
IMPACT PROPERTIES	55
DISCUSSION	58
OPTICAL MICROSCOPY	58
TRANSMISSION ELECTRON MICROSCOPY AND PRECIPITATE IDENTIFICATION	61
HEAT TREATMENT STUDIES	67
Austenitizing Studies	67
Tempering Studies	68
ELIMINATION OF DELTA-FERRITE FROM 12Cr-2WV STEEL	70
TENSILE PROPERTIES	71
IMPACT PROPERTIES	74
SUMMARY AND CONCLUSIONS	75
ACKNOWLEDGMENTS	78
REFERENCES	78

LIST OF FIGURES

<u>No.</u>	<u>Page</u>
1 Microstructure of low-chromium normalized-and-tempered 15.9-mm-thick plate: (a) 2.25CrV, (b) 2.25Cr-1WV, (c) 2.25Cr-2W, and (d) 2.25Cr-2WV steels	10
2 Microstructure of high-chromium normalized-and-tempered 15.9-mm-thick plate (a) 5Cr-2WV, (b) 9Cr-2WV, (c) 9Cr-2WVTa, and (d) 12Cr-2WV steels	11
3 Transmission electron microscopy photomicrographs of (a) 2.25CrV and (b) 2.25Cr-1WV steels showing examples of fibrous (a) and interphase (b) precipitation in the polygonal ferrite along with the bainitic structure of each steel	13
4 Transmission electron microscopy photomicrographs of the bainitic microstructures of (a) 2.25Cr-2W and (b) 2.25Cr-2WV steels	14
5 Transmission electron microscopy photomicrographs of the lath-martensite microstructure of 5Cr-2WV steel	15
6 Transmission electron microscopy photomicrographs of the lath martensite microstructure of (a) 9Cr-2WV and (b) 9Cr-2WVTa steels	16
7 Transmission electron microscopy photomicrographs of the lath-martensite and delta-ferrite microstructure of 12Cr-2WV steel	18
8 Extraction replica that show examples of the different precipitates that occur in normalized-and-tempered (a) 2.25CrV and (b) 2.25Cr-1WV steels	19
9 Examples of different types of precipitate observed on the extraction replica of normalized-and-tempered 2.25CrV steel: (a) fine fibers, (b) coarse fibers or "ribbons," (c) interphase precipitates, and (d) blocky precipitates	20
10 Extraction replica of normalized-and-tempered 2.25Cr-2W steel showing (a) the general precipitate distribution and (b) the fine distribution of precipitates at higher magnification	21
11 Extraction replica of normalized-and-tempered 2.25Cr-2WV steel showing (a) general precipitate distribution and (b) the distribution of fine precipitates at higher magnification	22

<u>No.</u>		<u>Page</u>
12	Extraction replica of normalized-and-tempered 5Cr-2WV steel	23
13	Extraction replicas of normalized-and-tempered (a) 9Cr-2WV and (b) 9Cr-2WVTa steels	24
14	Extraction replica of normalized-and-tempered 12Cr-2WV steel	25
15	Phase compositions tentatively identified as (a) M_3C and (b) M_2C_3 , as determined on extraction replica of 2.25Cr-1WV steel	30
16	A comparison of the fine precipitates in 2.25Cr-2WV and 2.25Cr-2W steels as shown by foil specimens in (a) and (b), by extraction replicas in (c) and (d), and by XEDS in (e) and (f). (a), (c), and (e) are the 2.25Cr-2WV and (b), (d), and (f) are the 2.25Cr-2W	31
17	Rockwell hardness plotted against austenitizing temperature for eight experimental heats. Specimens were cooled in flowing helium gas after 0.5 h at the austenitizing temperature	33
18	Rockwell hardness plotted against tempering temperature for 15.9-mm-thick plates of the eight experimental steels. Steels were normalized (N) and then tempered 2 h at 600, 650, 700, 750, and 780°C	34
19	Rockwell hardness plotted against the Hollomon-Jaffee tempering parameter for the 15.9-mm-thick plates of eight experimental steels. These data were obtained by tempering each steel for 2 h and then an additional 8 h at 600, 650, 700, 750, and 780°C. Also shown is a curve for 2.25Cr-1Mo steel	36
20	Microhardness (DPH) plotted against the tempering temperature for 15.9-mm-thick plates of the eight experimental steels. Steels were normalized (N) and pieces were tempered for 2 h at 600, 650, 700, 750, and 780°C	38
21	Microhardness plotted against the Hollomon-Jaffee tempering parameter for the 9Cr-2WV, 9Cr-2WVTa, 12Cr-2WV, 9Cr-1MoVNb, and 12Cr-1MoVW steels	40

<u>No.</u>		<u>Page</u>
22	Rockwell hardness plotted against tempering temperature for the 12Cr-2WV (0.1% C, 0.4% Mn) steel and three steels obtained from this composition by adjusting the manganese and carbon content. Specimens were tempered 2 h at the 600, 650, 700, 750, and 780°C	42
23	Tensile properties as a function of temperature for the 2.25Cr steels tempered at 700°C: (a) 0.2% yield stress, (b) ultimate tensile strength, and (c) total elongation	45
24	Tensile properties as a function of temperature for the 2.25Cr steels tempered at 750°C: (a) 0.2% yield stress, (b) ultimate tensile strength, and (c) total elongation	46
25	Tensile properties as a function of temperature for the 5, 9, and 12Cr steels tempered at 700°C: (a) 0.2% yield stress, (b) ultimate tensile strength, and (c) total elongation	48
26	Tensile properties as a function of temperature for the 5, 9, and 12Cr steels tempered at 750°C: (a) 0.2% yield stress, (b) ultimate tensile strength, and (c) total elongation	49
27	Tensile properties as a function of temperature for the 2.25Cr-2WV, 9Cr-2WV, and 9Cr-2WVTa steels tempered at 700°C: (a) 0.2% yield stress, (b) ultimate tensile strength, and (c) total elongation	51
28	Tensile properties as a function of temperature for the 2.25Cr-2WV, 9Cr-2WV, and 9Cr-2WVTa steels tempered at 750°C: (a) 0.2% yield stress, (b) ultimate tensile strength, and (c) total elongation	52
29	A comparison of tensile properties for 2.25CrV, 2.25Cr-1WV, 2.25Cr-2W, and 2.25Cr-2WV steels with 2.25Cr-1Mo steel: (a) 0.2% yield stress, (b) ultimate tensile strength, and (c) total elongation. Steels were normalized and then tempered for 1 h at 700°C	53
30	A comparison of the tensile properties for 2.25Cr-2WV, 9Cr-2WV, and 9Cr-2WVTa steels—the strongest Cr-W steels—with the properties for 9Cr-1MoVNb and 12Cr-1MoVW steels: (a) 0.2% yield stress, (b) ultimate tensile strength, and (c) total elongation. Steels were normalized and then tempered 1 h at 750°C	54

<u>No.</u>		<u>Page</u>
31	The Charpy V-notch impact curves for 2.25CrV, 2.25Cr-1WV, 2.25Cr-2W, and 2.25Cr-2WV steels; all steels were tempered for 1 h at 750°C	57
32	The Charpy V-notch impact curves for 5Cr-2WV, 9Cr-2WV, 9Cr-2WVTa, and 12Cr-2WV steels; all steels were tempered for 1 h at 750°C	59
33	A comparison of the Charpy V-notch impact curves for 9Cr-2WVTa and 12Cr-2WV steels with the curves for 9Cr-1MoVNb and 12Cr-1MoWV steels; all steels were tempered 1 h at 750°C	60
34	A comparison of the phase compositions for $M_{23}C_6$ in (a) 9Cr-1MoVNb and (b) 9Cr-2WV steels as determined on extraction replicas by XEDS; the $M_{23}C_6$ in the 9Cr-2WVTa steel was similar	65
35	The compositions of the MC phase as determined on extraction replicas by XEDS in (a) 2.25Cr-2WV, (b) 9Cr-2WV, (c) 9Cr-2WVTa, and (d) 9Cr-1MoVNb steels	66

LIST OF TABLES

<u>No.</u>		<u>Page</u>
1	Proposed nominal compositions for fast induced-radioactivity decay steel development program	4
2	Composition of fast induced-radioactivity decay ferritic steels	6
3	Identification of precipitates by X-ray diffraction and analytical electron microscopy	28
4	Tensile properties of normalized-and-tempered low-chromium steels	43
5	Tensile properties of normalized-and-tempered high-chromium steels	44
6	Impact properties of fast induced-radioactivity decay steels	56

DEVELOPMENT OF FERRITIC STEELS FOR FUSION REACTOR APPLICATIONS

R. L. Klueh, P. J. Maziasz, and W. R. Corwin

ABSTRACT

Chromium-molybdenum ferritic (martensitic) steels are leading candidates for the structural components for future fusion reactors. However, irradiation of such steels in a fusion environment will produce long-lived radioactive isotopes that will lead to difficult waste-disposal problems. Such problems could be reduced by replacing the elements in the steels (i.e., Mo, Nb, Ni, N, and Cu) that lead to long-lived radioactive isotopes. We have proposed the development of ferritic steels analogous to conventional Cr-Mo steels, which contain molybdenum and niobium. It is proposed that molybdenum be replaced by tungsten and niobium be replaced by tantalum.

Eight experimental steels were produced. Chromium concentrations of 2.25, 5, 9, and 12% were used (all concentrations are in wt %). Steels with these chromium compositions, each containing 2% W and 0.25% V, were produced. To determine the effect of tungsten and vanadium, 2.25Cr steels were produced with 2% W and no vanadium and with 0.25% V and 0 and 1% W. A 9Cr steel containing 2% W, 0.25% V, and 0.07% Ta was also studied. For all alloys, carbon was maintained at 0.1%.

Tempering studies on the normalized steels indicated that the tempering behavior of the new Cr-W steels was similar to that of the analogous Cr-Mo steels. Microscopy studies indicated that 2% tungsten was required in the 2.25Cr steels to produce 100% bainite in 15.9-mm-thick plate during normalization. The 5Cr and 9Cr steels were 100% martensite, but the 12Cr steel contained about 75% martensite with the balance delta-ferrite.

Precipitate types in the alloys varied, depending on the chromium content. For the 2.25Cr steels, M_3C and M_7C_3 were the primary precipitates; for the 9Cr and 12Cr steels, $M_{23}C_6$ was the primary precipitate. The 5Cr steel contained M_3C_3 and $M_{23}C_6$. All steels with vanadium also contained VC .

Tensile studies indicated that the 2.25Cr-2W-0.25V and 9Cr-2W-0.25V-0.07Ta steels had the highest strengths; they had properties similar to those of the 9Cr-1MoVNb and 12Cr-1MoVW steels that are candidates for fusion reactor applications. The 5Cr-2W-0.25V and 9Cr-2W-0.25V-0.07Ta steels had the best impact properties. The impact properties of these two steels as well as those of the 9Cr-2W-0.25V and 12Cr-2W-0.25V steels were comparable to the properties of similarly heat-treated Cr-Mo steels that are candidates for fusion reactor applications.

INTRODUCTION

The safety and environmental concerns that can result from the radioactivity induced in the first wall and blanket structure of a fusion reactor during its service lifetime have been discussed.¹ One problem involves the disposal of the highly radioactive blanket and first-wall structures after service. To simplify the waste-disposal procedures, the use of "low-activation" or "reduced-activation" steels (or other alloys) as structural materials has been proposed.¹ Such alloys should meet the guidelines issued by the U.S. Nuclear Regulatory Commission (10 CFR Part 61)² for shallow land burial, instead of the much more expensive deep geologic disposal. Decay to low levels for such alloys would occur in tens of years instead of hundreds or thousands of years.

As stated above, steels with such radioactivity decay characteristics are often referred to as "low-activation" or "reduced-activation" steels. Neither of these terms adequately describes the behavior of the steels during or after irradiation. When irradiated in a fusion reactor, all steels will become highly radioactive (i.e., activated). However, it is the radioactive decay characteristics with time after irradiation that are important for the steels under discussion.

The new steels to be developed to meet the above criteria will be compositionally modified so they contain only elements that produce radioactive isotopes that decay to low levels in a reasonable time. Therefore, we have chosen to call them "fast" induced-radioactivity decay (FIRD) steels.³ "Fast" is a relative term taken to mean that the radioactive transmutation products formed during irradiation in a fusion reactor decay rapidly enough to qualify for the shallow land burial techniques prescribed in 10 CFR Part 61 (see ref. 2).

Ferritic steels now being considered in the United States for fusion reactor applications are the following commercial Cr-Mo steels: 2.25Cr-1Mo (2.25% Cr-1% Mo-0.1% C*), 9Cr-1MoVNb (9% Cr-1% Mo-0.2% V-0.06% Nb-0.1% C),

* Throughout this report, concentrations are given in weight percent.

and 12Cr-1MoVW (12% Cr-1% Mo-0.25% V-0.5% W-0.5% Ni-0.2% C) steels. Molybdenum and niobium are the primary alloying elements that keep these steels from meeting the criteria for near-surface burial, and these elements would need to be eliminated. In fact, niobium would have to be reduced to extremely low residual levels.¹ Other normal alloying elements that must be minimized include nickel, copper, and nitrogen,¹ none of which play a significant role in determining the properties of the Cr-Mo steels under discussion, although 0.5% Ni is added to 12Cr-1MoVW steel to avoid delta-ferrite.

Because tungsten behaves like molybdenum in simple steels,⁴ it was proposed as a replacement for molybdenum.³ Vanadium has also been proposed as a replacement.⁵⁻⁷ To replace the strengthening function of niobium, the use of vanadium, titanium, and especially tantalum,⁸ which has chemical characteristics in common with niobium, have been suggested. Tantalum may cause problems, however, because its transmutation products produce high levels of radioactivity immediately after fission reactor irradiation, which make such steels difficult to study (fission reactor irradiation is presently the principal means of studying property changes caused by irradiation).

A series of experimental steels was previously proposed (Table 1),³ and in this report the results of the initial studies on those alloys will be presented. Designations to be used for the steels are given in Table 1 (e.g., 2.25CrV is used to designate the steel with 2.25% Cr and 0.25% V, etc.).

Compositions for these new steels were based on variations of the compositions of the three commercial ferritic steels currently of interest in the fusion reactor materials program. A range of chromium compositions from ~2.25 to 12% was proposed. An atom-for-atom replacement of molybdenum by tungsten was chosen; this required ~2% W, since the atomic weight of tungsten is approximately twice that of molybdenum. Vanadium was maintained at 0.25%, similar to the amount used in the Cr-Mo steels. Alloys with 2.25Cr and 0, 1, and 2% W were examined to determine the effect of tungsten, and an alloy with tungsten and no vanadium was examined to determine the effect of these elements on properties.

Table 1. Proposed nominal compositions for fast induced-radioactivity decay steel development program

Alloy	Nominal chemical composition ^a (wt %)				
	Cr	W	V	Ta	C
2.25CrV	2.25		0.25		0.1
2.25Cr-1WV	2.25	1	0.25		0.1
2.25Cr-2W	2.25	2			0.1
2.25Cr-2WV	2.25	2	0.25		0.1
5Cr-2WV	5	2	0.25		0.1
9Cr-2WV	9	2	0.25		0.1
9Cr-2WVTa	9	2	0.25	0.12	0.1
12Cr-2WV	12	2	0.25		0.1

^aBalance iron.

Tantalum was added to a 9Cr-2WV steel to obtain a steel analogous to the 9Cr-1MoVNb steel. A carbon level of 0.1 to 0.15% was proposed³ for all steels to help ensure weldability. Of the Cr-Mo steels presently in the program, only the 12Cr-1MoWV steel has more carbon. That steel contains 0.2% C which, along with 0.5% Ni, is used to eliminate delta-ferrite in this high-chromium alloy.

Programs to develop "reduced- or low-activation" ferritic steels are in progress throughout the world.⁵⁻¹⁰ In most of those programs, tungsten is used to replace molybdenum, although vanadium is also being used.⁵⁻⁷ Most of the programs have limited their studies to only a few alloys with compositions between 8 and 12% Cr.⁷⁻¹⁰

The objective of the alloy development program to be discussed here is the production of steels with properties equivalent or superior to those of the 2.25Cr-1Mo, 9Cr-1MoVNb, and 12Cr-1MoWV steels. This report describes

the first phase of the development of such steels, and the information presented here is expected to lead to further compositional improvements. Although the initial compositions were chosen to obtain information on the effect of chromium, tungsten, and vanadium on the properties of the FIRD steels, such information from the Cr-W steels should also be helpful in understanding the Cr-Mo steels. Likewise, the information presently being developed on the Cr-Mo steels, especially on irradiated properties, should also be helpful in the development of the FIRD steels.

EXPERIMENTAL PROCEDURE

Eight heats of steel* with the proposed nominal compositions given in Table 1 were prepared by Combustion Engineering, Inc., Chattanooga, Tennessee. Melt compositions are given in Table 2. In addition to the elements of primary interest (Cr, V, W, C, and Ta), other elements such as Mn, P, Si, etc., were adjusted to composition levels typically found in commercial steels.

All of the heats were air melted and then electroslag remelted (ESR) to obtain about 18 kg of usable material. The ESR ingot was hot rolled to 15.9- and 3.2-mm-thick plates. The 15.9-mm plates were heat treated and used for making standard Charpy V-notch specimens to determine the impact behavior. The 3.2-mm plate was further rolled into 0.76-mm sheet for the fabrication of tensile specimens.

The steels are projected to be used as fusion first-wall and blanket components in a normalized-and-tempered condition. By definition, a normalized steel is one that is air cooled after austenitization. The 15.9-mm-thick plate was given such a heat treatment. However, the heat treatments of the 0.76-mm sheet material and tensile specimens were

*As a generic designation, the new class of steels will be referred to as Cr-W steels. (The only exception is the 2.25CrV steel, which contains no tungsten.) This follows the procedure used for the Cr-Mo steels, after which these steels are patterned, even though both types of steel may contain other alloying elements.

Table 2. Composition of fast induced-radioactivity decay ferritic steels

Element	Chemical composition ^a (wt %)							
	2.25Cr-0.25V heat 3785	2.25Cr-1W-0.25V heat 3786	2.25Cr-2W heat 3787	2.25Cr-2W-0.25V heat 3788	5Cr-2W-0.25V heat 3789	9Cr-2W-0.25V heat 3790	9Cr-2W-0.25VTa heat 3791	12Cr-2W-0.25V heat 3792
C	0.11	0.10	0.11	0.11	0.13	0.12	0.10	0.10
Mn	0.40	0.34	0.39	0.47	0.47	0.51	0.43	0.46
P	0.015	0.015	0.016	0.016	0.015	0.014	0.015	0.014
S	0.006	0.006	0.005	0.006	0.005	0.005	0.005	0.005
Si	0.17	0.13	0.15	0.20	0.25	0.25	0.23	0.24
Ni	0.01	0.01	<0.01	<0.01				
Cr	2.36	2.30	2.48	2.42	5.00	8.73	8.72	11.49
Mo	0.01	<0.01	<0.01					
V	0.25	0.25	0.009	0.24	0.25	0.24	0.23	0.23
Nb	<0.01	<0.01	<0.01					
Ta	<0.01	<0.01	<0.01				0.075	
Ti	<0.01	<0.01	<0.01					
Co	0.005	0.006	0.008					
Cu	0.02	0.025	0.03					
Al	0.02	0.02	0.02	0.021	0.03	0.03	0.03	0.028
B	<0.001	<0.001	0.001					
W		0.93	1.99	1.98	2.07	2.09	2.09	2.12

^aBalance iron.

carried out in a helium atmosphere and cooled by pulling the specimens into the cold zone of the tube furnace. Because the cooling in helium is as fast or faster than air cooling, this heat treatment will also be referred to as normalizing.

Microstructures and heat treatment characteristics were determined on specimens taken from both the 0.76-mm-thick sheet and from the 15.9-mm-thick plate.

To determine the optimum austenitization temperature, a series of 0.76-mm-thick specimens was normalized by austenitizing 0.5 h at 900, 950, 1000, and 1050°C and then cooling in flowing helium. These specimens were subsequently annealed 2 h at 600, 650, 700, 750, and 780°C to determine the tempering characteristics of the steels given the different austenitizing treatments. Changes due to the heat treatments were determined by hardness measurements.

For tempering studies on the 15.9-mm-thick plate material, the 2.25Cr-2W steel was normalized by annealing 1 h at 900°C and air cooling. The other seven heats were annealed 1 h at 1050°C and air cooled; the higher temperature was used for these steels to assure that any vanadium carbides present were dissolved during the austenitization. Hardness determinations were made on each of the normalized steels and after pieces of the plate were tempered for 2 h at 600, 650, 700, 750, and 780°C. The hardness of each piece of steel was also determined after it was tempered an additional 8 h at the temperature used for the 2-h anneal.

Tensile tests were made on specimens with a reduced gage section 20.3 mm long by 1.52 mm wide by 0.76 mm thick. All specimens were machined with gage lengths parallel to the rolling direction. Tests were made in vacuum on a 120-kN-capacity Instron universal testing machine at a nominal strain rate of $4.2 \times 10^{-4}/s$.

For the impact tests, full-size Charpy-V-notch specimens were used. These were made from the 15.9-mm-thick plate in accordance with ASTM specification E 23 with dimensions of 10 mm by 10 mm by 55 mm; the specimens contained a 2-mm-deep, 45° V-notch with a 0.25-mm-root radius.

All specimens were taken along the rolling direction with the notch running transverse to the rolling direction (L-T orientation). Individual Charpy data sets were fitted to a hyperbolic tangent function for obtaining the transition temperature and upper-shelf energy.

Similar normalizing and tempering treatments were used on the tensile specimens and the plates from which the impact specimens were taken. All but the 2.25Cr-2W steel were austenitized at 750°C; the 2.25Cr-2W steel was austenitized at 900°C. The 15.9-mm plates were austenitized for 1 h, and the 0.76-mm tensile specimens were austenitized for 0.5 h. Two tempering treatments were tested: 1 h at 700°C and 1 h at 750°C. The only exception to these tempering temperatures was for the 2.25Cr-1WV steel, which was tempered for 1 h at 725°C and 1 h at 750°C. The plates were heat treated in air, and the tensile specimens were heat treated in helium.

Microstructures of the steels after various heat treatments were studied by optical microscopy, transmission electron microscopy (TEM), and analytical electron microscopy. Electron microscopy studies were conducted on specimens cut from tested impact specimens (the portion unaffected by the test). Thin foils and replicas were examined with a JEOL 100C microscope, and precipitate compositions were analyzed on a Philips EM 400T microscope and/or a JEOL 2000FX microscope using X-ray energy-dispersive spectroscopy (XEDS). The EM 400T was equipped with a field-emission gun that allows a fine, high-intensity electron probe for analysis of the smallest-detectable precipitates on the replicas (1-10 nm).

Precipitate phases were identified by a combination of electron diffraction and characteristic XEDS compositional analysis. To avoid matrix effects during XEDS analysis, precipitates were extracted on carbon-coated copper or nylon grids. For identification by X-ray diffraction, precipitates were electrolytically extracted from bulk samples with an approximate mass of 0.3 g. Extraction was in a solution of 10% HCl-90% methanol at 1.5 V for 5 h to determine their weight fraction. These solutions ensured selective removal of the matrix without any dissolution of carbides. Extracted precipitates were weighed to determine the percent precipitate in the steel. The accuracy of the extraction results was

determined by a series of multiple measurements on similar material. A value for 2 sigma of about 0.2 wt % was found.

RESULTS

OPTICAL MICROSCOPY

Specimens from the 15.9-mm-thick plates were examined by optical microscopy after normalizing (austenitized 1 h at 1050°C, except for the 2.25Cr-2W, which was austenitized 1 h at 900°C) and after normalizing and tempering at 700 and 750°C. Figures 1 and 2 show the microstructures after being normalized and tempered for 2 h at 700°C. The only effect of the tempering treatment on the optical microstructures was to produce visible carbides in the structures. In this section, the carbides will be ignored, since quantitative observations of carbides were not possible by optical microscopy.

Microstructures of the 2.25Cr steels contained bainite and polygonal or proeutectoid ferrite. The 2.25CrV alloy [Fig. 1(a)] had 30 to 35% bainite, with the remainder being ferrite. For the composition with 1% W—the 2.25Cr-1W steel—the microstructure contained ~55% bainite and 45% ferrite [Fig. 1(b)]. The 2.25Cr-2W [Fig. 1(c)] and 2.25Cr-2WV [Fig. 1(d)] steels contained bainite with much less polygonal ferrite: the 2.25Cr-2W steel was essentially 100% bainite; the 2.25Cr-2WV steel contained 15-20% polygonal ferrite.

The 5Cr-2WV [Fig. 2(a)], 9Cr-2WV [Fig. 2(b)], and 9Cr-2WVta [Fig. 2(c)] steels were 100% martensite. However, the 12Cr-2WV steel contained approximately 25% delta-ferrite, with the balance being martensite [Fig. 2(d)]. The only major difference in the martensite of these four steels was that the 9Cr-2WVta had a much finer prior austenite grain size [Fig. 2(c)].

Optical microstructures were also examined for the 0.76-mm-thick sheet after heat treatments similar to those used for the plates. All

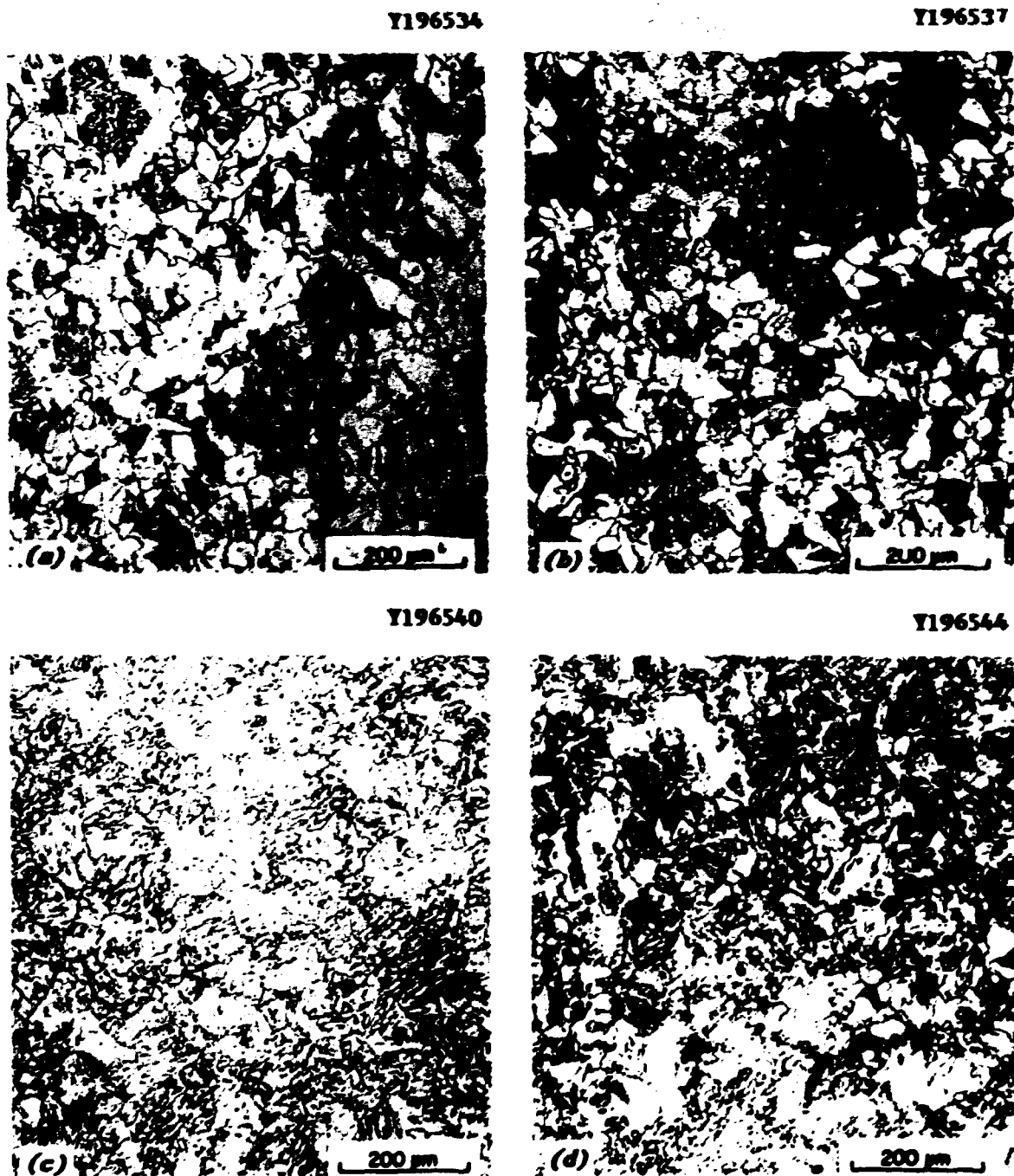


Fig. 1. Microstructure of low-chromium normalized-and-tempered 15.9-mm-thick plate: (a) 2.25CrV, (b) 2.25Cr-1WV, (c) 2.25Cr-2W, and (d) 2.25Cr-2WV steels.

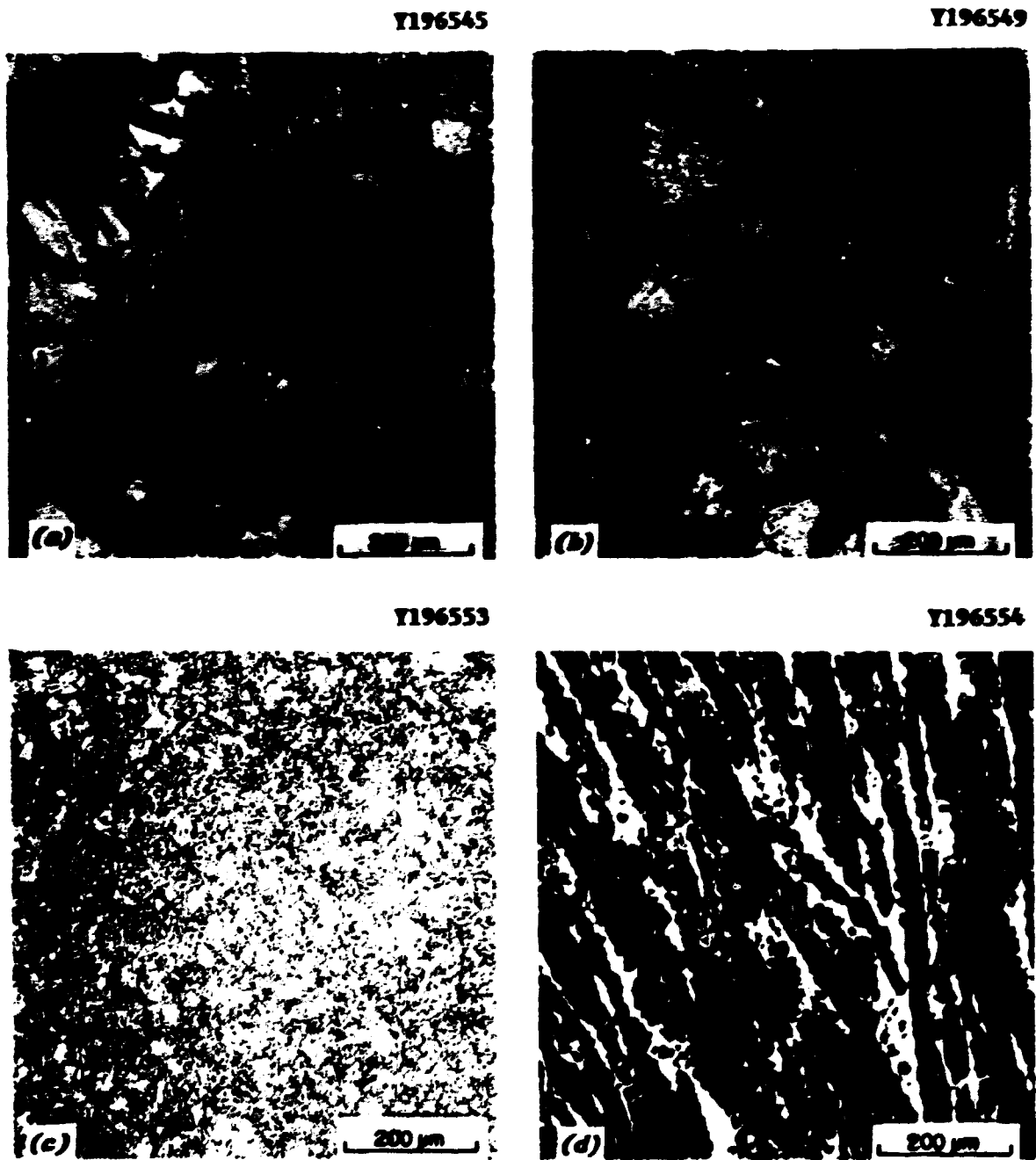


Fig. 2. Microstructure of high-chromium normalized-and-tempered 15.9-mm-thick plate: (a) 5Cr-2WV, (b) 9Cr-2WV, (c) 9Cr-2WVTa, and (d) 12Cr-2WV steel.

four of the 2.25Cr steels were entirely bainitic under these conditions, and the high-chromium steels had the same microstructures as found in the heat-treated plates.

TRANSMISSION ELECTRON MICROSCOPY

Transmission electron microscopy of the foil specimens showed a range of microstructures (Figs. 3 to 7). Figure 3 shows examples of fibrous [Fig. 3(a)] and interphase [Fig. 3(b)] precipitates. Such precipitates were observed in the polygonal ferrite regions of the 2.25CrV, 2.25Cr-1WV, and 2.25Cr-2WV steels and will be described more fully when the extraction replica results are presented. Also shown in Fig. 3 is the bainitic structure of the 2.25CrV [Fig. 3(a)] and the 2.25Cr-1WV [Fig. 3(b)] steels. Bainitic structures of the 2.25Cr-2W and 2.25Cr-2WV are shown in Fig. 4. These regions contained a high dislocation density, and some large precipitates were visible within these regions.

Lath-martensite structures were observed in the 5 to 12% Cr steels. The 5Cr steel appeared to contain considerable precipitate throughout the matrix as well as lath boundaries (Fig. 5). Microstructures of the 9Cr-2WV and 9Cr-2WVTa steels appeared to be quite similar (Fig. 6). The lath size of the 9Cr-2WVTa was probably slightly smaller than that of the 9Cr-2WV, but there was no large difference. The lath structure of the 12Cr-2WV steel was relatively fine, while the delta-ferrite of this steel contained a relatively high dislocation density and some precipitation (Fig. 7).

For a more detailed examination of the carbide structure of the normalized-and-tempered steel plate, carbide extraction replicas were analyzed. Figures 8 to 14 show the different types of carbide microstructures that were observed.

The 2.25CrV and 2.25Cr-1WV steels (Fig. 8) showed the most diverse microstructures. Both steels contained fibrous precipitates, interphase precipitates, and large blocky precipitates. As discussed later, the

YE-13642



YE-13648



Fig. 3. Transmission electron microscopy photomicrographs of (a) 2.25CrV and (b) 2.25Cr-1WV steels showing examples of fibrous (a) and interphase (b) precipitation in the polygonal ferrite along with the bainitic structure of each steel. The bainite is on the right side of each photograph.

YE-13650



YE-13680

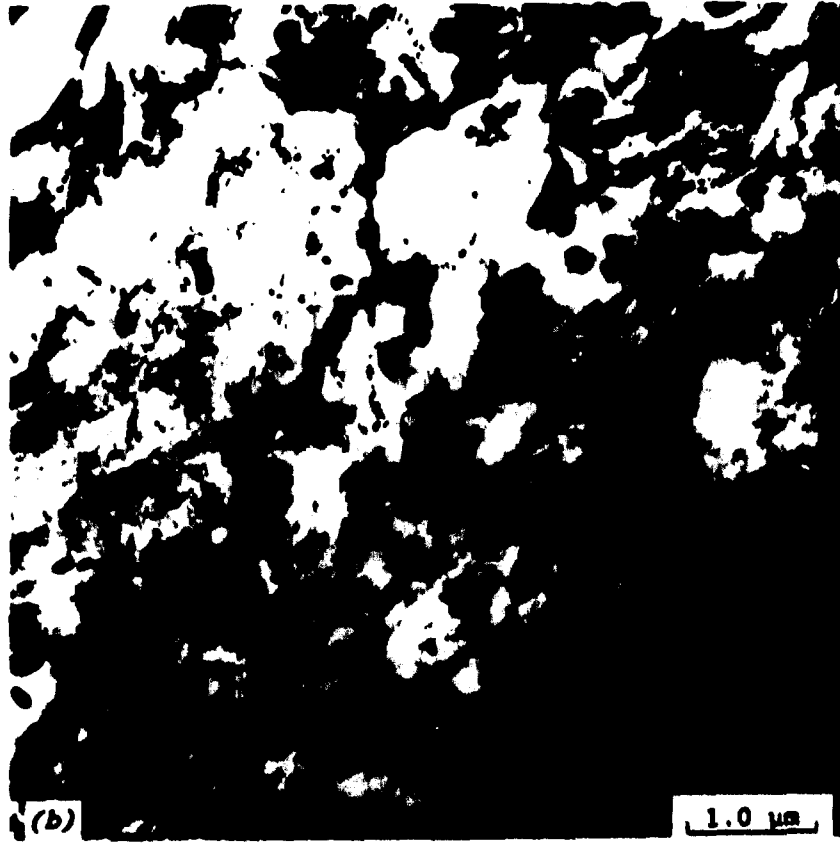


Fig. 4. Transmission electron microscopy photomicrographs of the bainitic microstructures of (a) 2.25Cr-2W and (b) 2.25Cr-2WV steels.

YE-13664



YE-13666

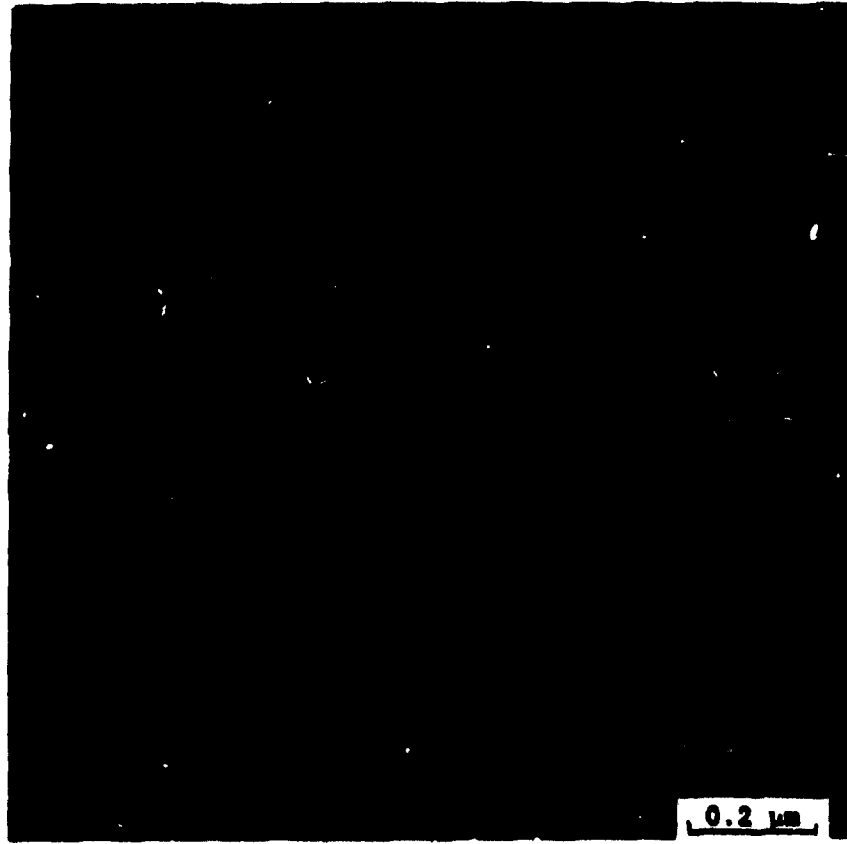


Fig. 5. Transmission electron microscopy photomicrographs of the lath-martensite microstructure of 5Cr-2WV steel.

(a)

YE-13667



YE-13668

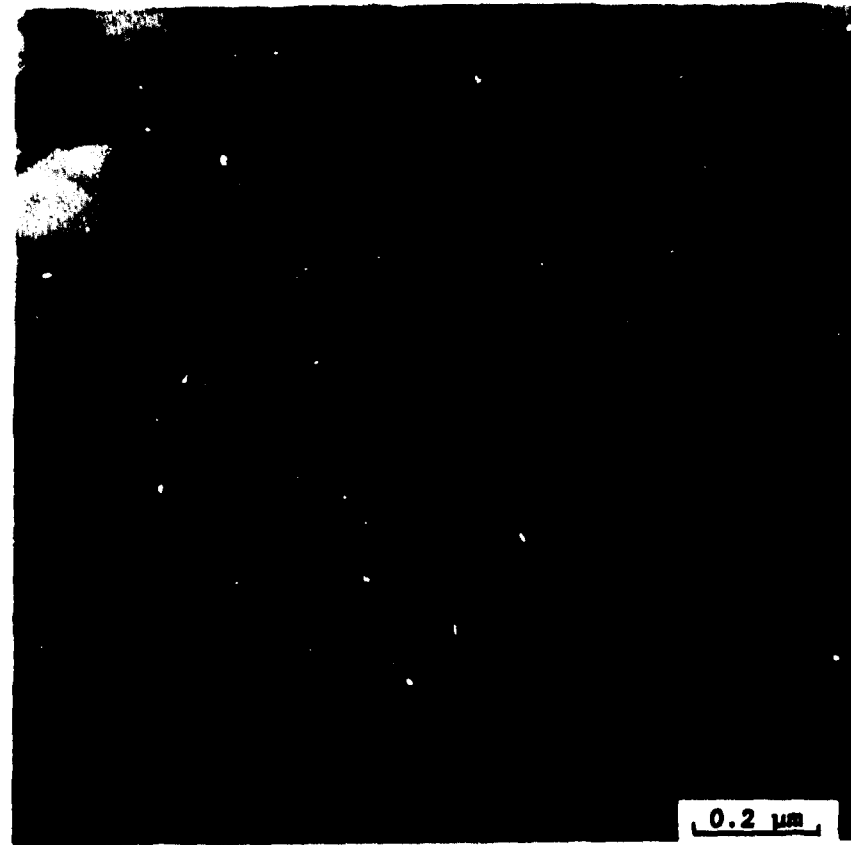
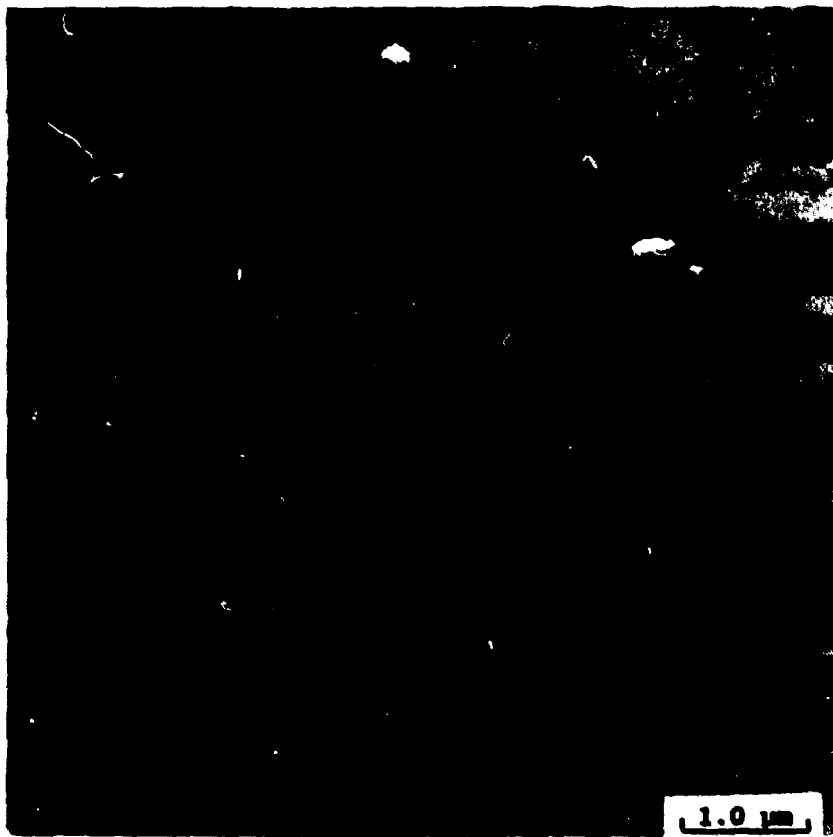


Fig. 6. Transmission electron microscopy photomicrographs of the lath-martensite microstructure of (a) 9Cr-2WV and (b) 9Cr-2WVTa steels.

(b)

YE-13670



YE-13671



17

Fig. 6. Continued.

YE-13672



YE-13674



Fig. 7. Transmission electron microscopy photomicrographs of the lath-martensite and delta-ferrite microstructure of 12Cr-2W steel.

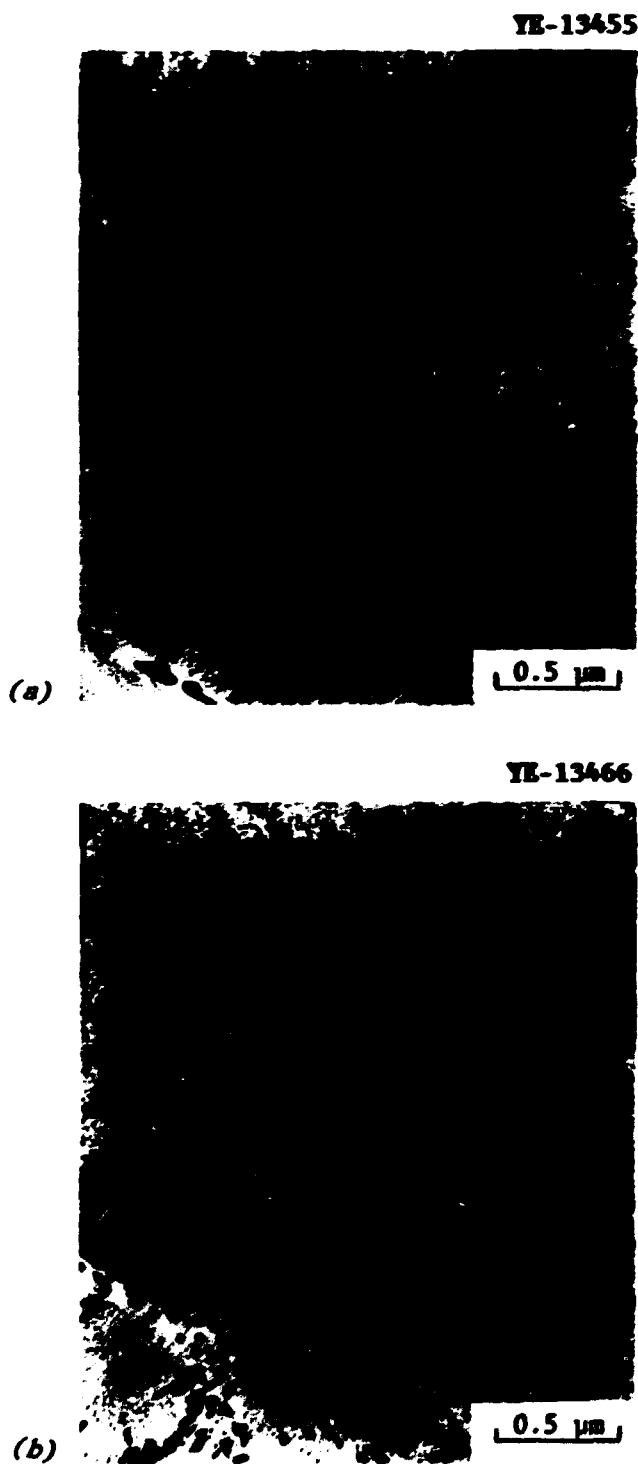


Fig. 8. Extraction replicas that show examples of the different precipitates that occur in normalized-and-tempered (a) 2.25CrV and (b) 2.25Cr-1WV steels.

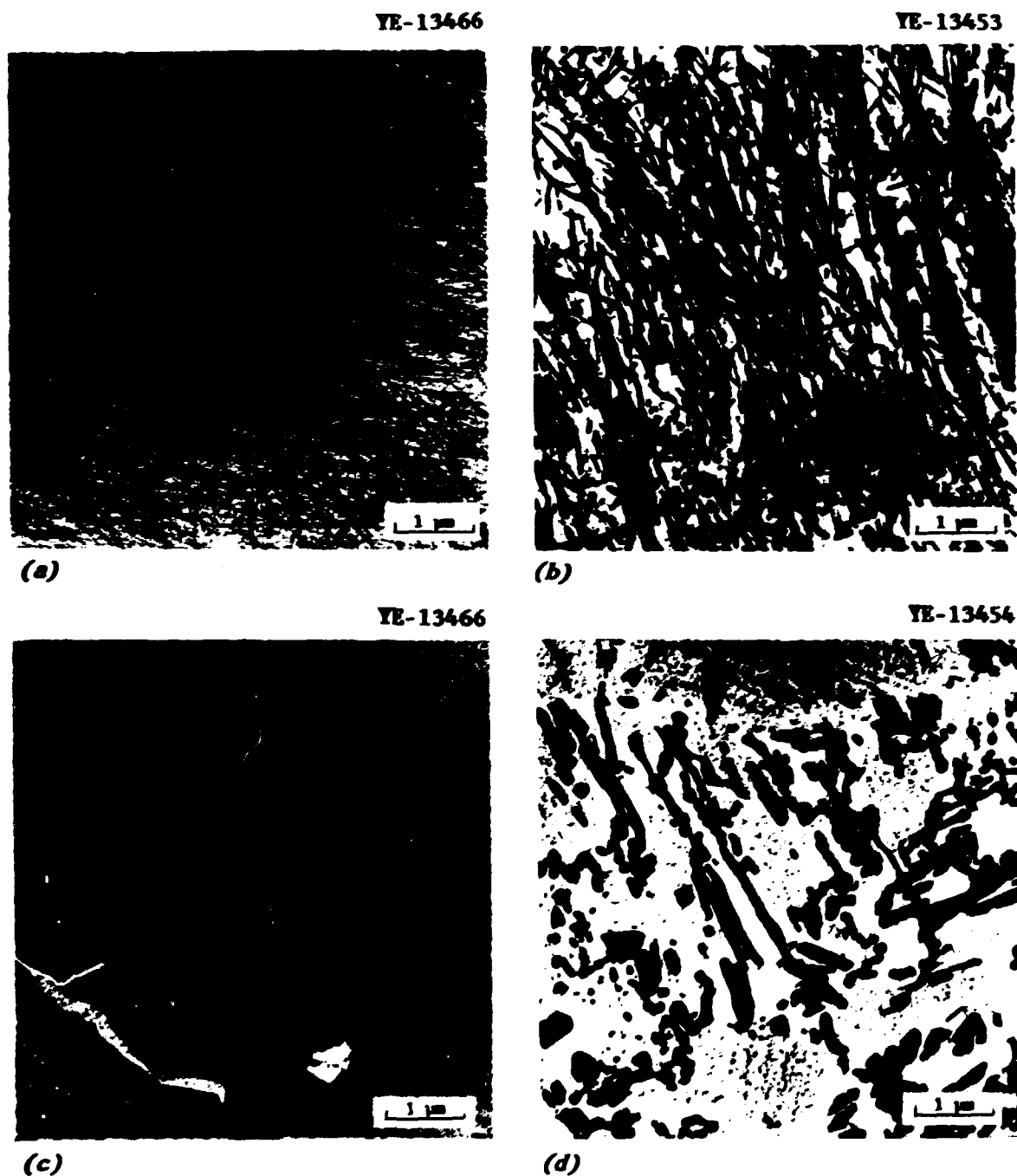


Fig. 9. Examples of different types of precipitate observed on the extraction replica of normalized-and-tempered 2.25CrV steel: (a) fine fibers, (b) coarse fibers or "ribbons," (c) interphase precipitates, and (d) blocky precipitates.

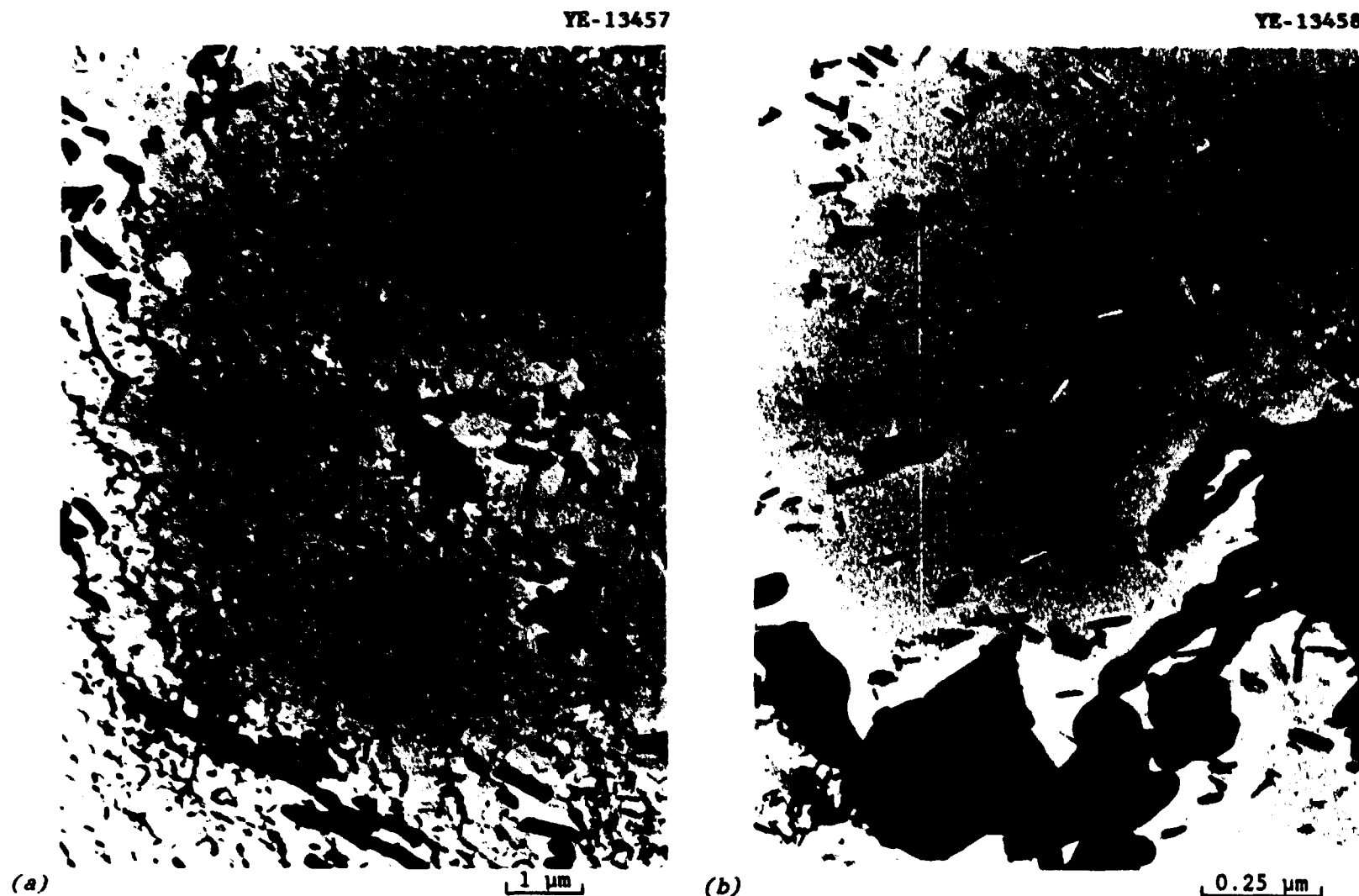


Fig. 10. Extraction replica of normalized-and-tempered 2.25Cr-2WV steel showing (a) the general precipitate distribution and (b) the fine distribution of precipitates at higher magnification.

YE-13459



YE-13460



Fig. 11. Extraction replica of normalized-and-tempered 2.25Cr-2WV steel showing (a) general precipitate distribution and (b) the distribution of fine precipitates at higher magnification.

YE-13462

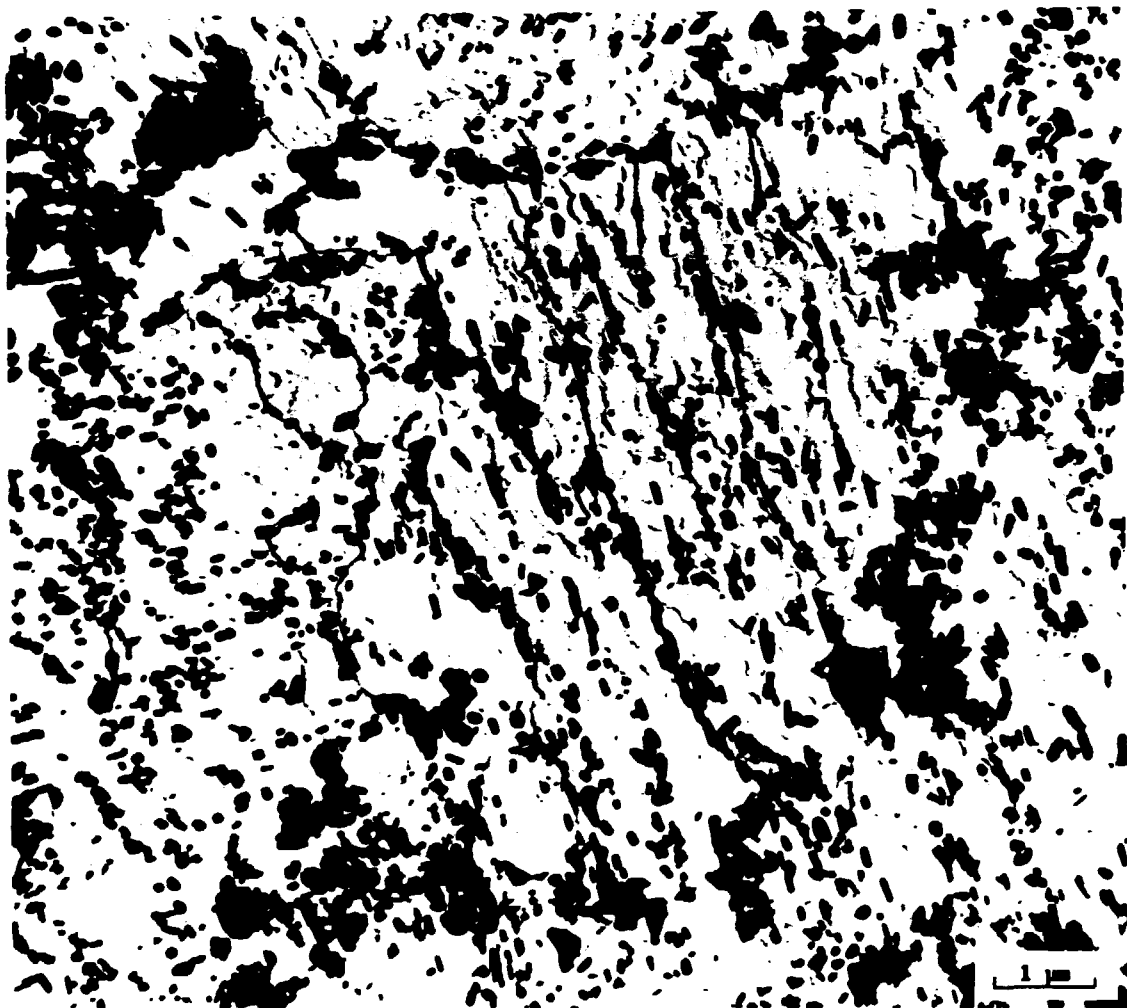
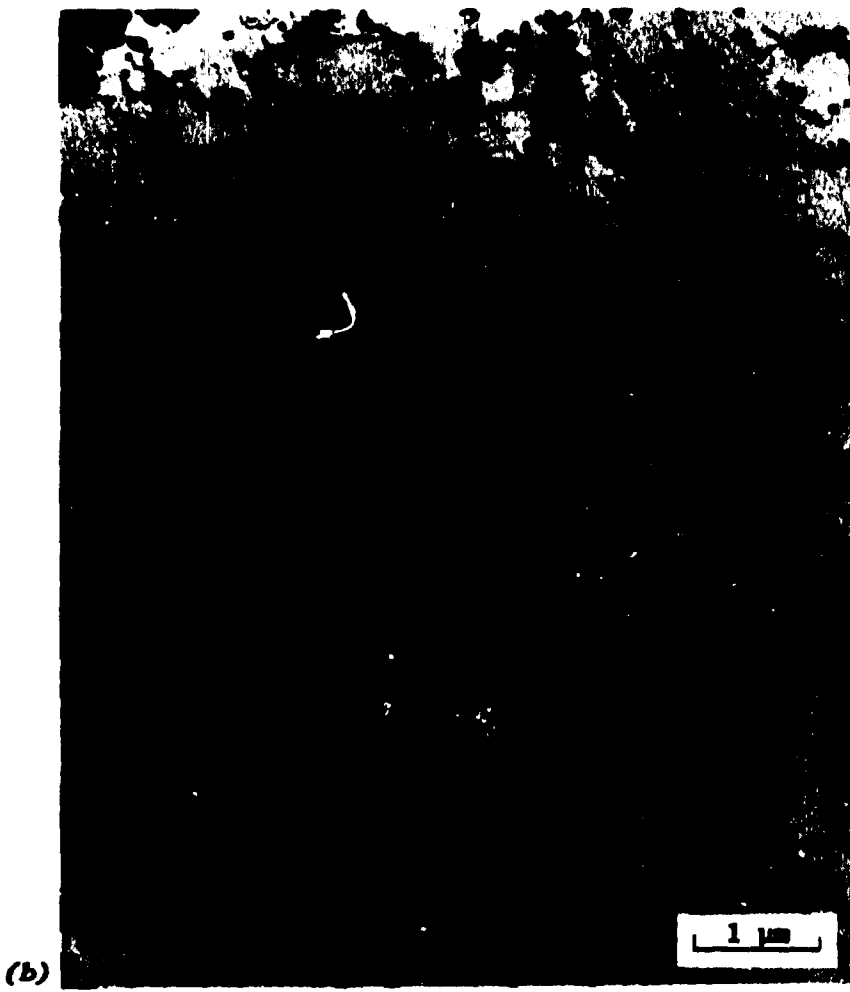


Fig. 12. Extraction replica of normalized-and-tempered 5Cr-2WV steel.

YE-13463



YE-13464



26

Fig. 13. Extraction replicas of normalized-and-tempered (a) 9Cr-2WV and (b) 9Cr-2WVTa steels.

YE-13465

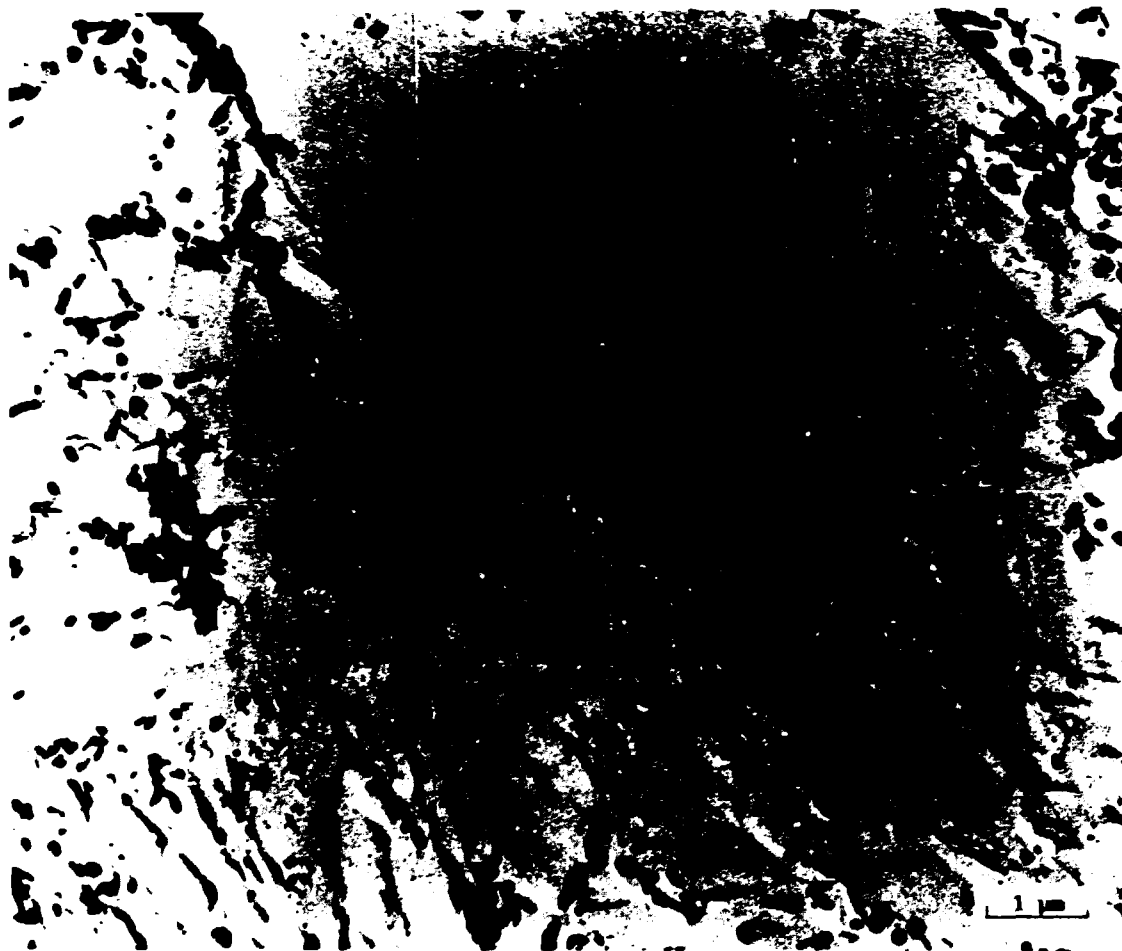


Fig. 14. Extraction replica of normalized-and-tempered 12Cr-2WV steel.

fibrous and interphase precipitates occurred in the polygonal ferrite. Fibrous precipitates are quite obvious in the micrographs of Figs. 8, 9(a), and 9(b). There were two types of fibers: the fine fibers that are illustrated in Figs. 8 and 9(a) and coarser fibers or "ribbons," as seen in Fig. 9(b). A morphological characteristic of the interphase precipitation is that it generally consists of rows of fine precipitates [Fig. 9(c)]. Large, blocky precipitates [Fig. 9(d)] appeared in two regions: along prior austenite grain boundaries and within regions of the bainitic matrix in which there were no fibrous or interphase precipitates. Fibrous precipitate in the 2.25Cr-1WV was finer than that in the 2.25CrV steel. The arrangement of the interphase precipitate into rows in the 2.25CrV steel was usually quite easily recognized, although in some instances the high density of precipitates made recognition difficult. Rows of precipitates were quite difficult to recognize in the 2.25Cr-1WV steel, where the precipitate was somewhat finer than that in the 2.25CrV steel.

As demonstrated in Fig. 9(c), the large precipitates in the bainitic matrix regions appeared in various shapes. On average, the coarse precipitates were smaller in the 2.25Cr-1WV steel than in the 2.25CrV steel. In general, the regions that contained large precipitates also contained a distribution of finer precipitate particles, although these particles were generally not as small and less abundant than the interphase precipitate particles. The 2.25Cr-1WV steel contained a higher density of these finer particles in the bainitic regions than did the 2.25CrV steel.

No fibrous or ribbon precipitates were observed in the 2.25Cr-2W steel, which optical microscopy showed to be entirely bainitic. It contained two types of precipitate: fine needlelike particles and large blocky particles (Fig. 10).

Only a few fibrous precipitates were observed in the 2.25Cr-2WV steel, which contained 15-20% polygonal ferrite. Some interphase precipitate regions were detected, but the particles were much smaller than those found in the 2.25CrV and 2.25Cr-1WV steels. The bainite of the 2.25Cr-2WV steel, like that of the 2.25Cr-2W steel, contained two types of

precipitate: large blocky particles and a high density of fine particles (Fig. 11). The blocky particles in the 2.25Cr-2WV were similar in appearance to those in the 2.25Cr-2W steel, but the fine particles were smaller and were present in much larger numbers. At high magnification [Fig. 11(b)], the small particles appeared to be a mixture of needlelike and rectangular (in two dimensions) morphologies.

As seen in Fig. 12, the size and spacial distributions of the precipitate particles in the 5Cr-2WV steel were different from those observed in the 2.25Cr steels. Most of the particles in the 5Cr-2WV steel had a blocky or rectangular morphology of quite uniform size. There were also precipitates of a somewhat larger size, many of which formed along prior austenite grain boundaries; others lay in fairly straight lines, indicating that they had formed on lath boundaries. Although not obvious from Fig. 12, fine particles could also be detected at higher magnification.

The 9Cr-2WV and 9Cr-2WVTa steels contained fairly large blocky precipitates (Fig. 13). Many of these precipitates appeared to have formed on lath boundaries or on prior austenite grain boundaries. At higher magnification fine precipitates could be detected in the matrix regions that appeared to be free of precipitates at lower magnification. The 12Cr-2WV steel had a similar microstructure, except for some grains that were free of coarse precipitates (Fig. 14). These are the delta-ferrite grains that constitute about 25% of the microstructure. It appeared that these grains contained some very fine precipitates.

PRECIPITATE IDENTIFICATION

By weighing the precipitate obtained by bulk electrolytic extraction, the amount of precipitate was determined (Table 3). Crystal structures of the extracted precipitates were analyzed by X-ray diffraction. The type of precipitate identified by X-ray diffraction depended on the chromium concentration of the steel. For the 9Cr and 12Cr steels, only $M_{23}C_6$ was positively identified. In the 2.25Cr steels, the detected precipitate appeared to depend on the vanadium and tungsten composition. When

Table 3. Identification of precipitates by X-ray diffraction^a and analytical electron microscopy^b

Steel	Precipitate (wt %) ^c	Tentative identification
2.25CrV	0.926	$M_3C + M_7C_3 + MC$
2.25Cr-1WV	1.059	$M_3C + M_7C_3 + MC$
2.25Cr-2W	1.797	$M_3C + M_7C_3 + M_{23}C_6 + M_2X$
2.25Cr-2WV	1.946	$M_3C + M_7C_3 + MC$
5Cr-2WV	2.299	$M_{23}C_6 + M_7C_3 + MC$
9Cr-2WV	2.520	$M_{23}C_6 + MC$
9Cr-2WVTa	2.033	$M_{23}C_6 + MC$
12Cr-2WV	2.037	$M_{23}C_6 + MC$

^aX-ray diffraction of the extracted precipitates.

^bX-ray energy-dispersive spectroscopy (XEDS) on extraction replicas.

^cObtained by weighing the extracted precipitates.

vanadium was present, the steels contained M_7C_3 , M_3C , and MC . The 2.25Cr-2W steel contained M_3C and $M_{23}C_6$. The 5Cr-2WV steel, which has an intermediate chromium concentration, contained $M_{23}C_6$ and M_7C_3 , which is a combination of the dominant chromium-rich phases found in the higher and the lower chromium alloys, respectively.

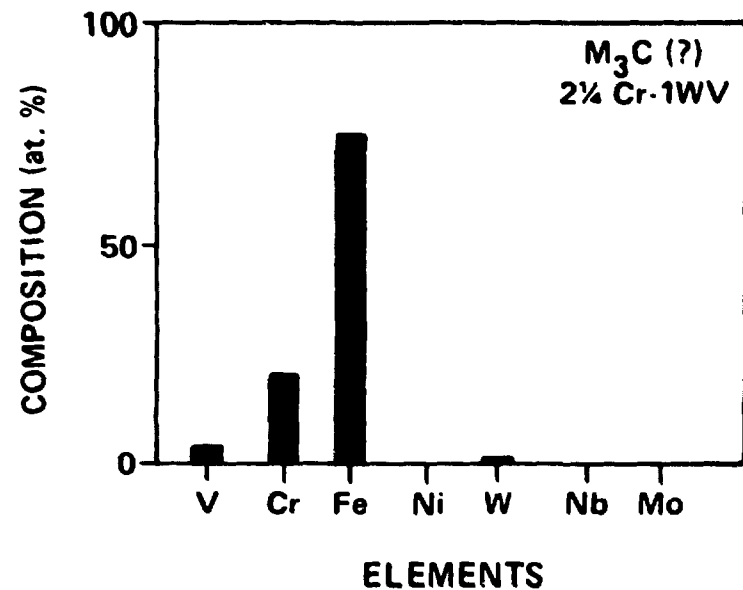
One problem with X-ray diffraction is that fine precipitates are difficult to positively identify. This caused unidentified X-ray diffraction lines for some specimens. Further, the overlap of lines for different compounds complicates positive identification. It became clear from the replica analyses discussed below that there were fine precipitate phases that were not identified by X-ray analysis.

To further identify the precipitates and to correlate them with morphology, carbide-extraction replicas were examined by XEDS. Analysis of the complicated microstructures of the 2.25CrV and 2.25Cr-1WV steels (Figs. 8 and 9) indicated that both the fine fibers and interphase precipitates were vanadium rich and were presumably MC. Both types of MC contained considerable amounts of chromium, with the fine fibers containing the most chromium. The coarse fibers or ribbons were iron and chromium rich, with slightly more iron than chromium. Presumably, these are M_2C_3 , since this carbide can contain large amounts of both iron and chromium. The large precipitates that formed in the bainite were mainly of two types: chromium rich and iron rich (Fig. 15). A broad beam analysis over a field of these precipitates revealed that the chromium-rich phase was probably the M_2C_3 phase, while the iron-rich particles were probably the M_3C phase, both of which were found by X-ray diffraction. A few large precipitates were found to be vanadium rich, presumably MC particles. Fine MC precipitates were also found.

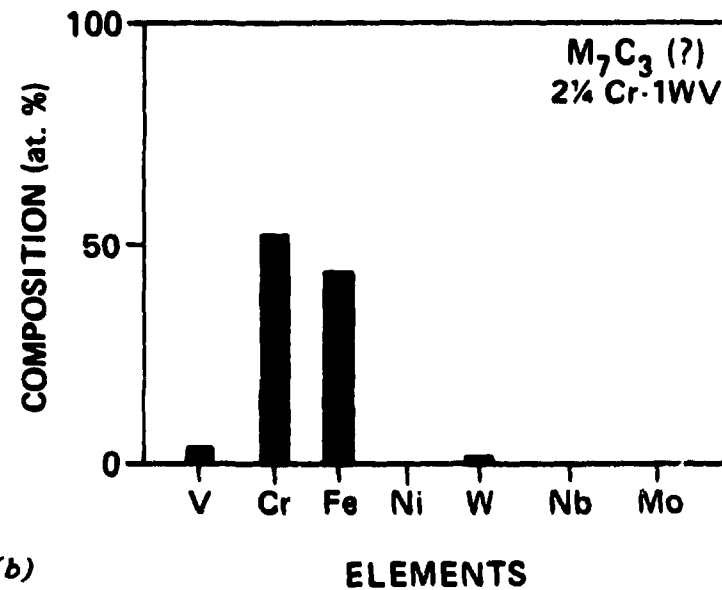
The large precipitates in the bainite of the 2.25Cr-2W and 2.25Cr-2WV steels were similar to those in the 2.25CrV and 2.25Cr-1WV: M_2C_3 and M_3C . No M_23C_6 was detected in the 2.25Cr-2W, even though it was observed by X-ray diffraction. The fine precipitates in the 2.25Cr-2W steel were different from those in the 2.25Cr-2WV steel (Fig. 16). In the 2.25Cr-2W steel, the fine needlelike precipitates were chromium and tungsten rich and were probably M_2C or M_2X . The fine precipitates in the 2.25Cr-2WV steel were MC particles. However, instead of being only vanadium rich, as was true for the 2.25CrV and 2.25Cr-1WV steels, the fine MC in this steel was also rich in tungsten (Fig. 16). Some of the larger particles in this steel were also vanadium- and tungsten-rich MC, and some were rich only in vanadium.

XEDS analysis of the large precipitates in the 5Cr-2WV steel showed them to be mainly M_2C_3 , while the very small particles were vanadium-rich MC. For the martensite of the 9Cr-2WV, 9Cr-2WVTa, and 12Cr-2WV, the precipitates were either M_23C_6 (large particles) or MC (small particles and a few of the large particles). In the 9Cr-2WV and 12Cr-2WV steels,

ORNL-DWG 87-13202A



(a)



(b)

Fig. 15. Phase compositions tentatively identified as (a) M_3C and (b) M_7C_3 , as determined on extraction replica of 2.25Cr-1WV steel.

ORNL PHOTO 4602-87

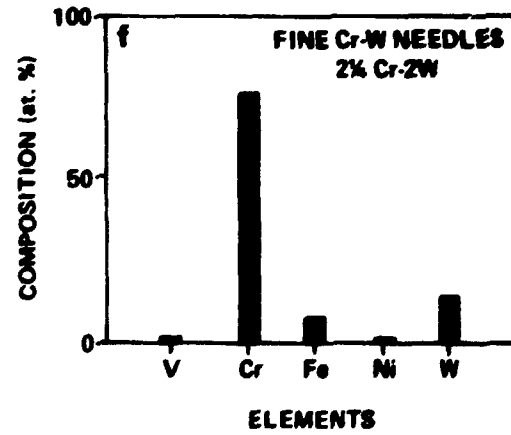
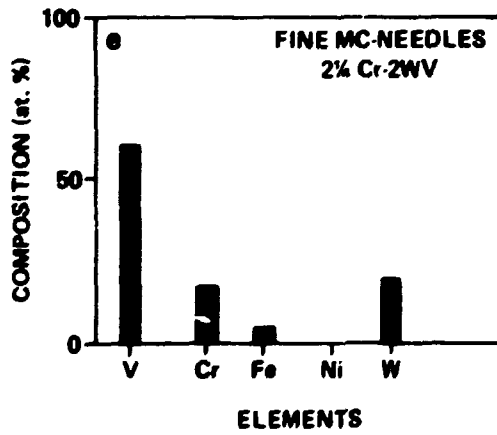
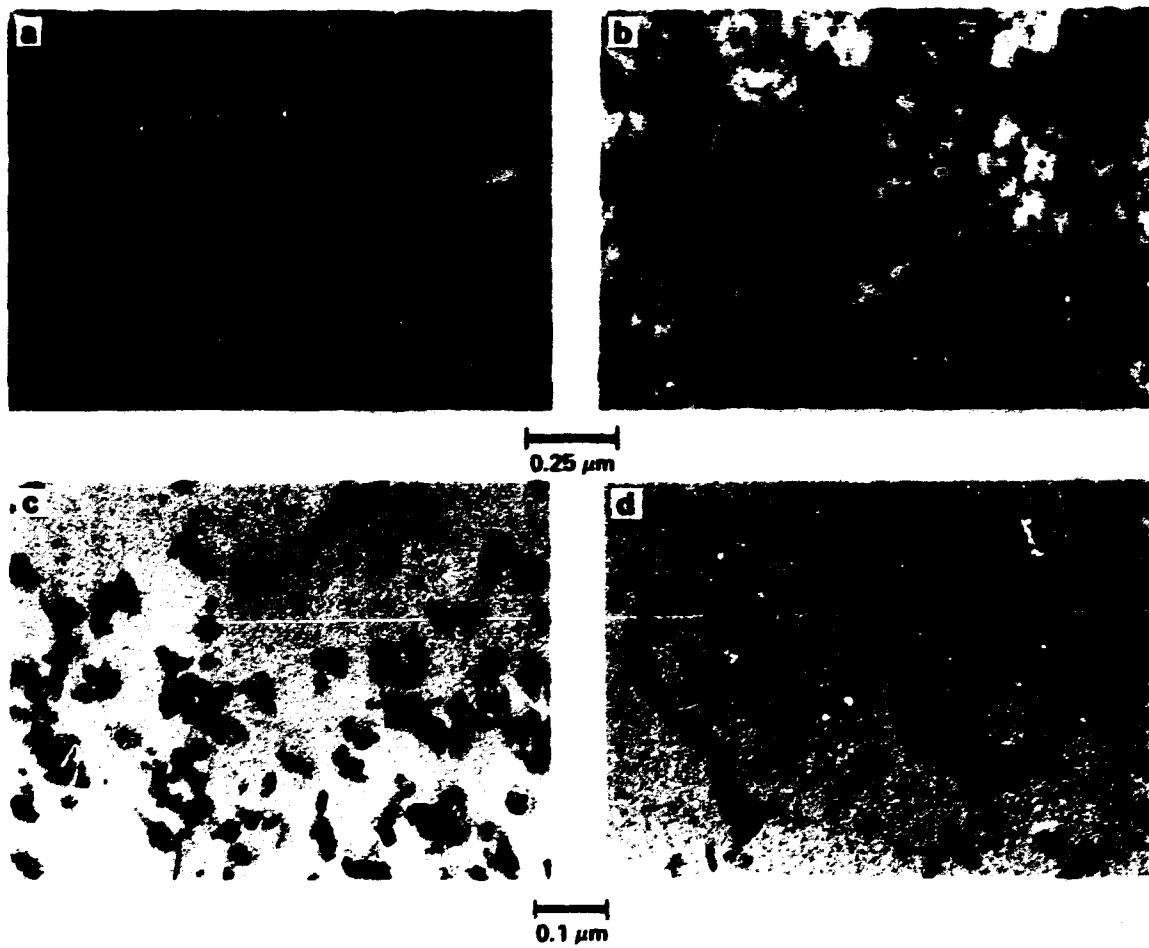


Fig. 16. A comparison of the fine precipitates in 2.25Cr-2WV and 2.25Cr-2W steels as shown by foil specimens in (a) and (b), by extraction replicas in (c) and (d), and by XEDS in (e) and (f). (a), (c), and (e) are the 2.25Cr-2WV and (b), (d), and (f) are the 2.25Cr-2W.

the MC was vanadium rich, with considerable chromium present (no large amounts of tungsten as found in the 2.25Cr-2WV steel). The 9Cr-2WVTa contained two types of MC: vanadium rich and tantalum rich, both of which contained considerable chromium.

Table 3 summarizes the precipitates that were found by X-ray diffraction and analytical electron microscopy.

HEAT TREATMENT STUDIES

Austenitizing Behavior

Figure 17 shows the effect of different austenitizing temperatures on the hardness of the normalized 0.76-mm-thick sheet. The hardnesses of the 2.25CrV and 2.25Cr-1WV steels increased with temperature and reached similar maximum hardnesses. Maximum hardness for the 2.25Cr-2W steel was reached with the 900°C anneal; a similar hardness was obtained after annealing at 950 and 1000°C, but decreased after annealing at 1050°C. The 2.25Cr-2WV steel developed the highest hardness of the 2.25Cr steels. A hardness peak was reached with the 1000°C anneal, although there was little change between 1000 and 1050°C.

Hardness changes for the higher chromium steels fell into two categories, with the 5Cr and 9Cr steels in one group, and the 12Cr steel in the other. The first group developed a maximum hardness between 950 and 1000°C, although there was only a small decrease when annealed at 1050°C (Fig. 17). A 950°C austenitizing treatment caused a large increase in the hardness of the 12Cr-2WV steel relative to that observed at 900°C; however, hardness increased only slightly at the higher temperatures.

Tempering Behavior

Tempering curves are given in Fig. 18 for the specimens taken from the 15.9-mm-thick plate and austenitized for 1 h at 900°C (the 2.25Cr-2W steel) or for 1 h at 1050°C (the other seven heats) and then air cooled. Data are for pieces of plate tempered 2 h at 600, 650, 700, 750, and 780°C; the normalized hardness is also shown. Although several heats displayed

ORNL-DWG 85C-16355

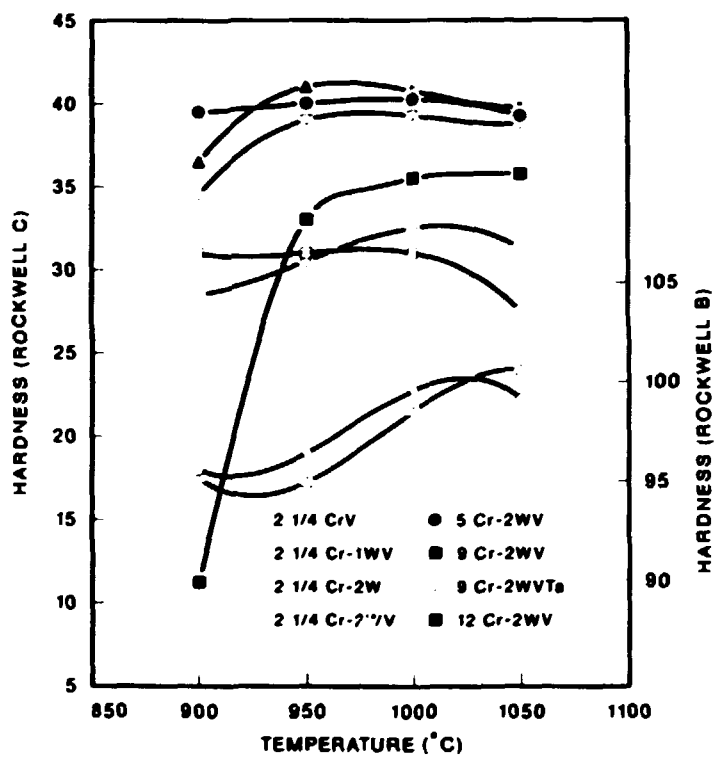


Fig. 17. Rockwell hardness plotted against austenitizing temperature for the eight experimental heats. Specimens were cooled in flowing helium gas after 0.5 h at the austenitizing temperature.

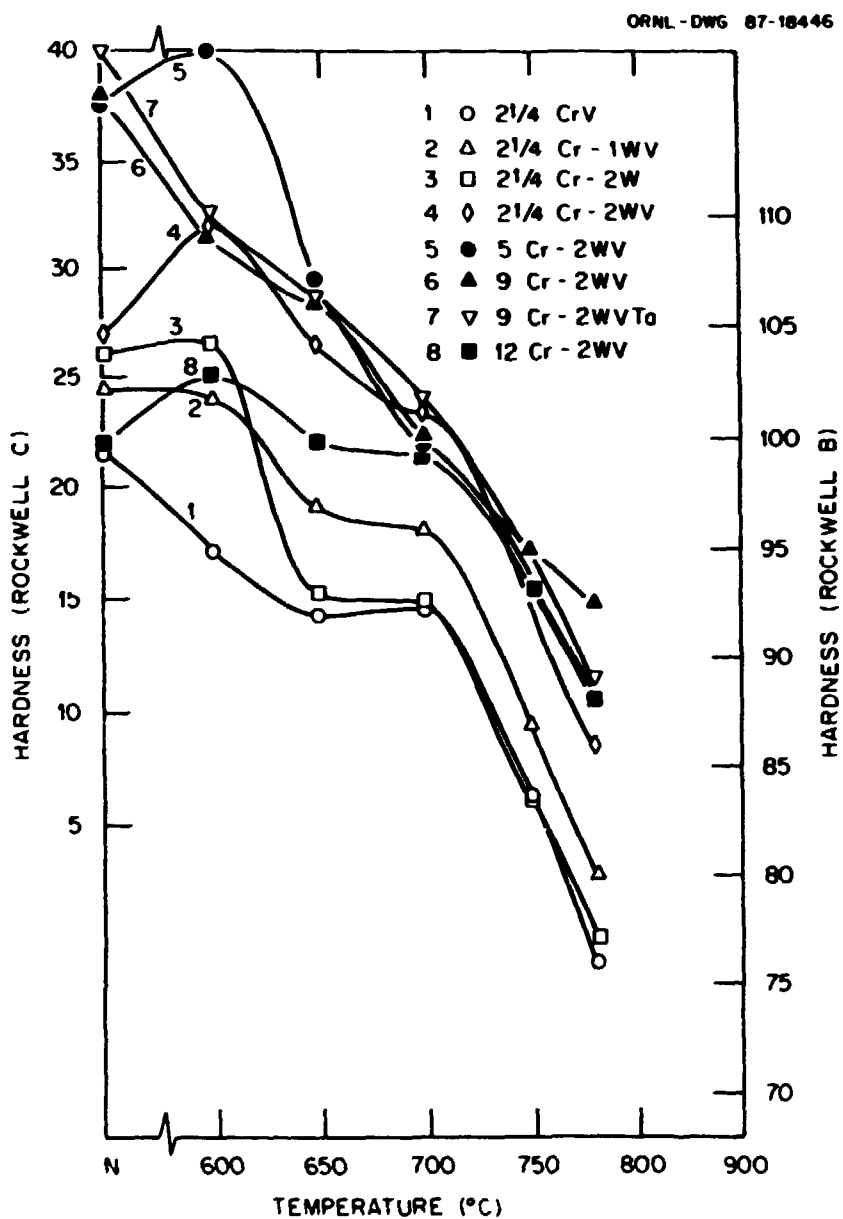


Fig. 18. Rockwell hardness plotted against tempering temperature for 15.9-mm-thick plates of the eight experimental steels. Steels were normalized (N) and then tempered 2 h at 600, 650, 700, 750, and 780°C.

secondary hardening peaks, all heats showed a continuous decrease in hardness when tempered above 600°C.

Tempering behavior for the 2.25Cr steels was affected by the presence of the tungsten and vanadium. Steels with 1 and 2% W and 0.25% V (2.25Cr-1WV and 2.25Cr-2WV) displayed increasing hardness with increasing tungsten content. The 2.25CrV steel (0.25% V without any tungsten) was clearly the softest. On the other hand, the 2.25Cr-2W steel (2% W but no vanadium) had higher hardness than either the 2.25CrV or the 2.25Cr-1WV steels after normalizing and after tempering at 600 and 650°C. After tempering at 650°C and above, the hardness of the 2.25Cr-2W was less than that of the 2.25Cr-1WV steel and approached that of the 2.25CrV steel.

Despite the fact that the 2.25Cr-2WV steel was not entirely bainite, the as-normalized hardness of the steel was similar to the hardness of the 2.25Cr-2W steel. After tempering, the 2.25Cr-2WV steel had the highest hardness of the 2.25Cr steels, regardless of the tempering conditions. Tempering for 2 h at 600°C produced maximum hardness for this steel, whereas, at the highest tempering temperature, this steel had a hardness similar to that of the high-chromium steels comparably tempered (Fig. 18).

The tempering behavior of the 5Cr-2WV steel was interesting, because after 2 h at 600°C the hardness approached the highest hardness achieved for any of these steels—similar to that for the as-normalized 9Cr-2WVTa steel. The two 9Cr steels showed little difference in tempering behavior: both had normalized hardnesses near R_C 40, but then the hardnesses decreased continuously with tempering temperature.

After tempering at 600 and 700°C, the 12Cr-2WV steel with only 75% martensite (balance delta-ferrite) had a lower hardness than the other steels that were entirely martensite. However, the tempering resistance of this steel was such that when tempered at 750 and 780°C the hardness approached that of the 5Cr and 9Cr steels, which contained no delta-ferrite.

In Fig. 19, the Rockwell hardness is plotted against the empirical Hollomon-Jaffee parameter, which attempts to account for the effect of both the time and the temperature used during the tempering treatment.

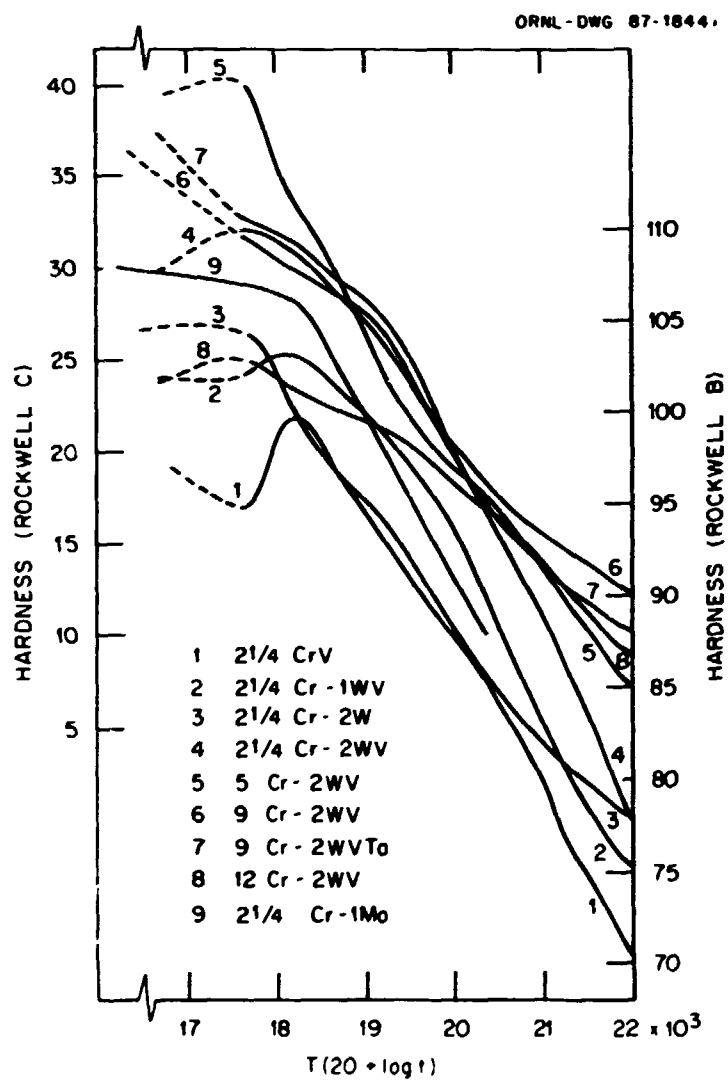


Fig. 19. Rockwell hardness plotted against the Hollomon-Jaffee tempering parameter for the 15.9-mm-thick plates of eight experimental steels. The data were obtained by tempering each steel for 2 h and then for an additional 8 h at 600, 650, 700, 750, and 780°C. Also shown is a curve for 2.25Cr-1Mo steel.

The parameter is defined as $T(20 + \log t)$, where T is the absolute temperature in K and t is tempering time in h. Hardnesses were determined for all the steels after 2 h at the five tempering temperatures and after being tempered for another 8 h at the same tempering temperature. Relative changes in hardness after a 10-h temper were consistent with those observed after 2 h but at different tempering temperatures (Fig. 18). After tempering to a parameter of -20×10^3 , there was relatively little hardness difference between the 2.25Cr-2WV, the 5Cr-2WV, the two 9Cr steels, and the 12Cr-2WV. For the larger values of the Hollomon-Jaffee parameter, the hardness of the 2.25Cr-2WV steel decreased somewhat faster than that of the high-chromium steels.

Microhardness measurements were made on metallography specimens of the 15.9-mm-thick plates tempered 2 h at each temperature and are plotted against tempering temperature in Fig. 20. As expected, the relative behavior was similar to that observed for Rockwell-hardness measurements (Fig. 18).

Pieces of the 0.76-mm-thick sheet given the different normalizing heat treatments shown in Fig. 17 were tempered for 2 h at 600, 650, 700, 750, and 780°C. Generally, for any given tempering treatment, the tempered hardness of a steel given a normalizing treatment that yielded a maximum hardness remained greater than that for the same steel given other normalizing treatments. The tempering behavior of the 5Cr, 9Cr, and 12Cr sheet material was similar to that observed on the thicker plate material (Fig. 18), when compared for similar normalizing treatments. The tempering behavior of the 2.25Cr steels was affected by section size: the plate material contained considerable amounts of proeutectoid ferrite that was not present in the normalized sheet material. Thus, the normalized sheet was harder, especially at lower tempering temperatures.

In this study, no Cr-Mo steels were heat treated for comparison. However, some tempering data for 2.25Cr-1Mo steel obtained under similar circumstances were available, and these data are shown in Fig. 19. It can be seen that the hardness of the 2.25Cr-1Mo steel is similar to the presently studied alloys--especially the 2.25Cr-2W steel at

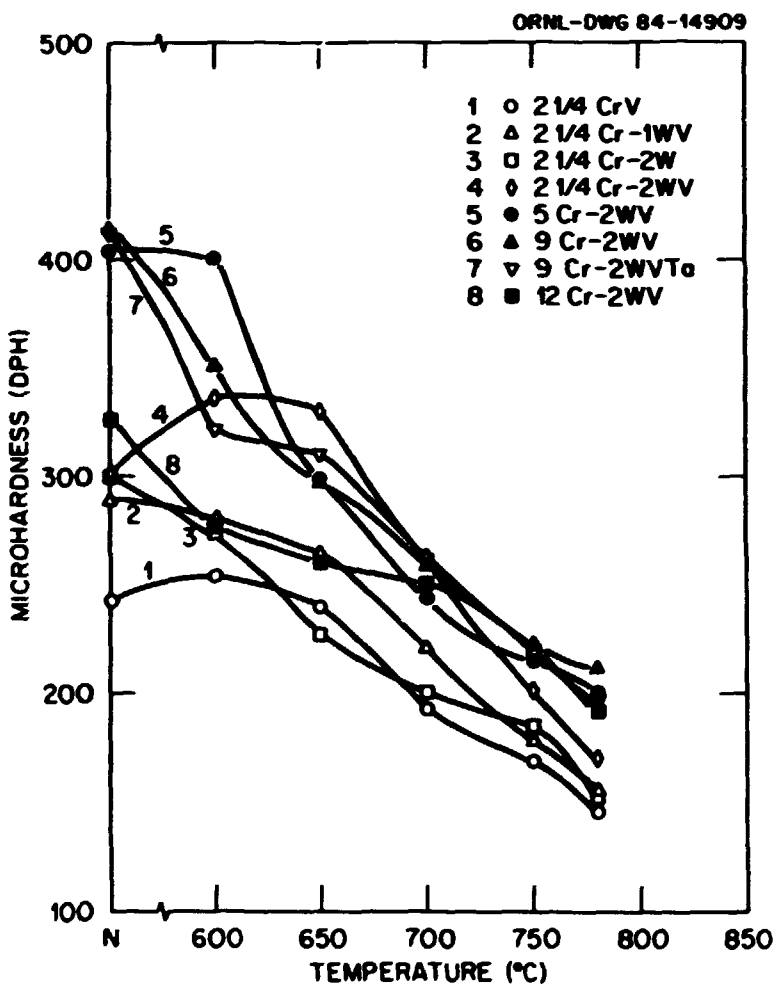


Fig. 20. Microhardness (DPH) plotted against the tempering temperature for 15.9-mm-thick plates of the eight experimental steels. Steels were normalized (N) and pieces were tempered for 2 h at 600, 650, 700, 750, and 780°C.

the higher tempering parameters. The 2.25Cr-1WV and 2.25Cr-2WV steels were more resistant to tempering than 2.25Cr-1Mo steel.

The only tempering studies made on the 9Cr-1MoVNb and 12Cr-1MoVW steels being studied in the fusion program were microhardness measurements on 0.76-mm-thick sheet.¹¹ These steels were entirely martensitic when normalized. Because cooling rate has little effect on the hardness of martensite,¹² a comparison can be made between the 9Cr and 12Cr Cr-Mo and Cr-W steels (Fig. 21). The 9Cr-2WV and 9Cr-2WVTa steels behaved like the 9Cr-1MoVNb steel. The 12Cr-2WV steel had a lower hardness at the lowest tempering parameter, but at long times it approached the values of the 9Cr steels. If the hardness values of the 2.25Cr-2WV and 5Cr-2WV steels were plotted on this curve, they would also compare favorably with the 9Cr steels. The 12Cr-1MoVW steel was harder than the 9Cr steels, presumably because it contained 0.2% C, compared to 0.1% C for the other steels.

ELIMINATION OF DELTA-FERRITE FROM 12Cr-2WV STEEL

When the 12Cr-1MoVW steel is normalized and tempered, it is essentially 100% martensite.¹¹ Because chromium, molybdenum, and tungsten promote the formation of delta-ferrite, 0.2% C and 0.5% Ni are used to offset the effect of these elements and promote austenite formation during austenitization. The 12Cr-2WV steel was produced with no nickel, because nickel must be minimized in FIRD steels. Carbon was maintained at 0.1% for good weldability. To eliminate delta-ferrite in a FIRD 12Cr steel, additional carbon can be added and manganese, an austenite stabilizer, can be used as a replacement for nickel.³

With the 12Cr-2WV steel as the base composition, three 400-g button heats were produced with 2.8% Mn, 5.6% Mn, and 0.2% C (the base composition contained ~0.5% Mn and 0.1% C). As opposed to the 0.5% Ni in the 12Cr-1MoVW steel, higher manganese concentrations were required because manganese is not as strong an austenite former as nickel.

Specimens ~6.4 mm thick were normalized by austenitizing for 0.5 h at 1050°C and then cooling in flowing helium. After that treatment, the

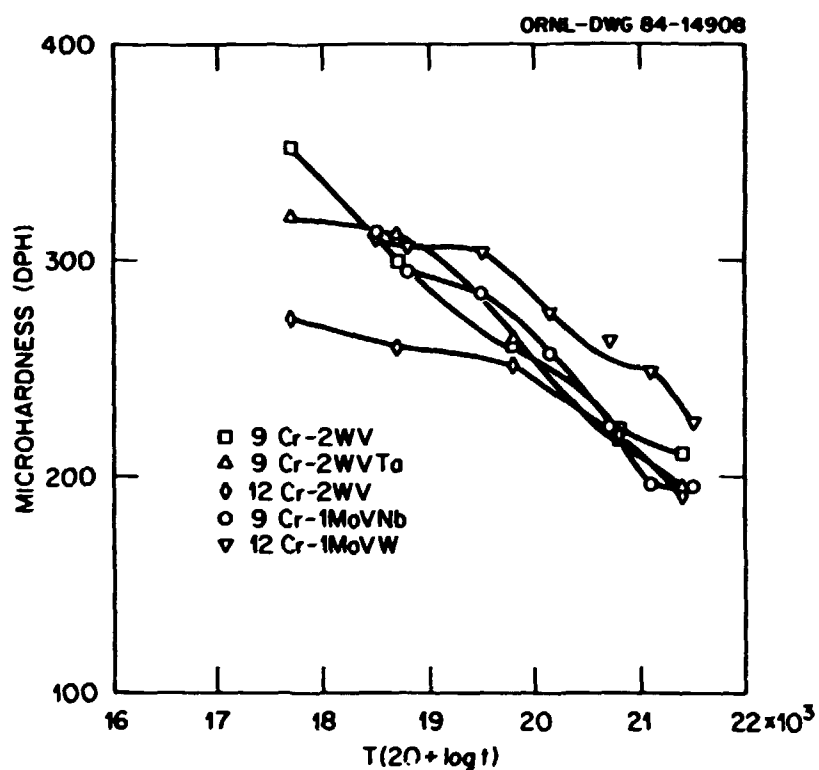


Fig. 21. Microhardness plotted against the Hollomon-Jaffee tempering parameter for the 9Cr-2WV, 9Cr-2WVTa, 12Cr-2WV, 9Cr-1MoVNb, and 12Cr-1MoVW steels.

2.8% Mn and 5.6% Mn steels contained ~10% and <1% delta-ferrite, respectively; the steel with 0.2% C contained ~5% delta ferrite. These values were considerably less than the 25% delta-ferrite in the base 12Cr-2WV steel.

To determine the tempering characteristics of the modified 12Cr-2WV steels, normalized (austenitized 0.5 h at 1050°C) 0.76-mm-thick sheet was tempered for 2 h at 600, 650, 700, 750, and 780°C. Hardness results are shown in Fig. 22, along with the results for the 12Cr-2WV steel. Results indicated that the steel with 0.2% C had the highest hardness at the low tempering temperatures. The hardnesses of the steels with 2.8 and 5.6% Mn went through a minimum--the first near 750°C and the second near 700°C. The steel with the 0.2% C had a higher hardness than either of the manganese-modified steels up to the temperature at which the minimum is reached. The hardness of the 12Cr-2WV steel approached that of the steel with 0.2% C and the one with 2.8% Mn at an intermediate tempering temperature (~700°C).

TENSILE PROPERTIES

Tensile tests were conducted over the temperature range from room temperature to 600°C on the 0.76-mm-thick specimens that were normalized and tempered. Normalizing involved austenitizing for 0.5 h at 1050°C, except for the 2.25Cr-2W steel, which was austenitized for 0.5 h at 900°C; steels were tested after tempering for 1 h at 700°C and for 1 h at 750°C. Tensile properties are given in Tables 4 and 5.

Data for the low-chromium (2.25% Cr) steels tempered at 700 and 750°C (Table 4) are plotted in Figs. 23 and 24, respectively, and data for the high-chromium (5 to 12% Cr) steels (Table 5) are plotted in Figs. 20 and 21, respectively. For all of the steels, the strength was substantially lower after tempering at 750°C than after tempering at 700°C. In general, the relative strengths of the different steels were the same after the two different tempering treatments.

OPNL-DWG 85G-10354

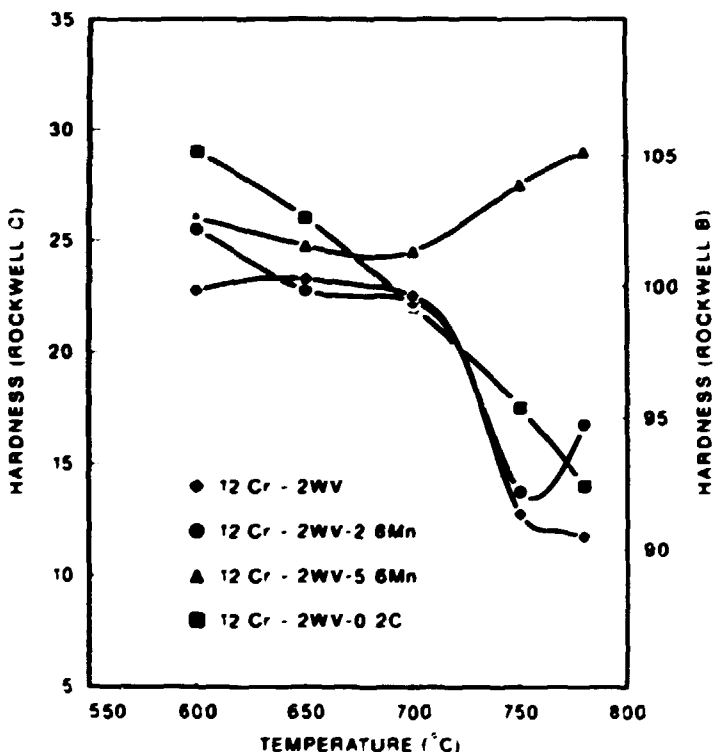


Fig. 22. Rockwell hardness plotted against tempering temperature for the 12Cr-2WV (0.1% C, 0.4% Mn) steel and three steels obtained from this composition by adjusting the manganese and carbon content. Specimens were tempered 2 h at 600, 650, 700, 750, and 780°C.

Table 4. Tensile properties of normalized-and-tempered low-chromium steels^a

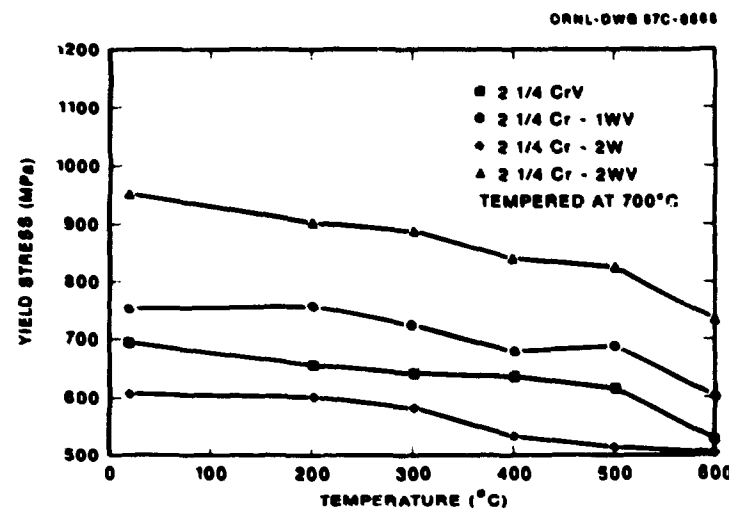
Tempered for 1 h at 700°C						Tempered for 1 h at 750°C					
Test temperature (°C)	Strength (MPa)		Elongation (%)			Test temperature (°C)	Strength (MPa)		Elongation (%)		
	Yield	Ultimate	Uniform	Total			Yield	Ultimate	Uniform	Total	
2.25 CrV											
22	674	733	4.4	7.6		22	557	640	5.9	9.4	
200	639	698	3.6	6.4		200	500	571	4.3	7.3	
300	621	697	3.1	6.0		300	496	582	5.1	8.1	
400	619	677	3.0	5.8		400	471	551	4.0	5.9	
500	599	658	2.6	5.6		500	472	552	3.0	6.4	
600	520	539	1.1	4.9		600	394	413	1.1	6.0	
2.25 Cr-1W											
22	727	763	4.3	6.3		22	579	653	6.6	8.8	
200	731	795	4.3	7.3		200	-	-	-	-	
300	694	755	3.3	5.8		300	527	608	4.8	7.9	
400	660	731	3.5	6.3		400	540	624	4.3	6.9	
500	659	726	2.9	5.9		500	504	589	3.3	6.4	
600	588	620	1.5	5.1		600	401	421	1.3	5.0	
2.25 Cr-2W											
22	594	668	6.1	9.5		22	554	618	9.6	13.5	
200	588	654	5.9	9.3		200	542	581	8.1	12.0	
300	573	628	5.3	8.0		300	531	570	7.1	10.0	
400	526	631	4.8	7.8		400	474	555	6.9	9.9	
500	509	635	5.5	8.6		500	430	609	7.4	10.4	
600	501	576	3.6	7.6		600	372	484	4.6	9.1	
2.25 Cr-2WV											
22	904	964	5.3	8.5		22	649	719	6.3	10.0	
200	860	925	5.0	8.0		200	625	692	5.8	9.1	
300	848	911	4.1	7.0		300	620	698	5.0	7.9	
400	803	882	3.4	6.6		400	583	671	4.9	8.0	
500	789	871	3.5	6.4		500	571	674	4.6	8.0	
600	768	760	1.9	5.6		600	528	588	2.8	6.4	

^aAll but the 2.25Cr-2W steel were austenitized for 0.5 h at 1050°C; the 2.25Cr-2W was austenitized for 1 h at 900°C.

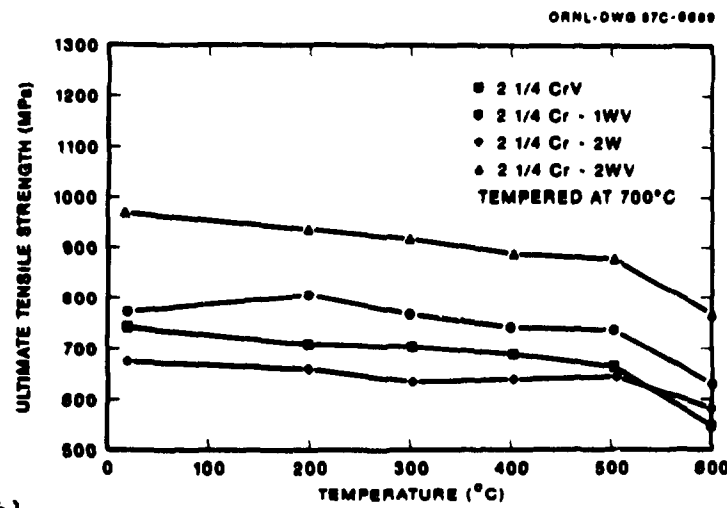
Table 5. Tensile properties of normalized-and-tempered high-chromium steels^a

Tempered for 1 h at 700°C						Tempered for 1 h at 750°C					
Test temperature (°C)	Strength (MPa)		Elongation (%)			Test temperature (°C)	Strength (MPa)		Elongation (%)		
	Yield	Ultimate	Uniform	Total			Yield	Ultimate	Uniform	Total	
5Cr-2WV											
22	715	811	4.5	8.0		22	577	703	6.0	9.9	
200	695	784	3.6	6.8		200	551	664	4.9	8.8	
300	673	756	3.3	6.6		300	524	635	4.5	8.1	
400	676	753	2.8	5.5		400	517	611	3.8	7.0	
500	629	706	2.0	4.6		500	484	583	3.4	6.3	
600	538	565	1.2	5.6		600	440	497	2.5	7.3	
9Cr-2WV											
22	790	910	4.4	7.5		22	597	725	5.5	9.0	
200	760	865	3.4	6.5		200	573	699	4.4	7.8	
300	710	825	3.3	6.1		300	675	675	4.1	7.4	
400	711	797	2.6	5.4		400	540	621	3.3	6.1	
500	660	734	1.9	4.3		500	531	626	2.4	5.1	
600	599	644	1.6	6.3		600	463	530	2.1	6.0	
9Cr-2WVta											
22	823	942	3.8	6.6		22	645	714	3.3	7.9	
200	-	-	-	-		200	611	727	3.8	6.9	
300	782	873	2.8	5.0		300	606	709	3.4	6.5	
400	761	840	2.3	5.0		400	585	682	2.9	5.9	
500	707	779	1.6	4.1		500	538	615	2.1	4.6	
600	651	696	1.4	4.8		600	489	526	1.6	5.9	
12Cr-2WV											
22	708	859	5.4	8.4		22	606	757	5.8	9.0	
200	668	804	4.5	7.5		200	589	724	5.0	8.3	
300	649	777	4.4	7.4		300	557	688	4.3	7.4	
400	650	703	3.4	6.1		400	524	646	3.6	6.4	
500	601	698	2.5	5.0		500	506	601	2.6	5.1	
600	500	528	2.3	6.6		600	427	488	2.5	6.1	

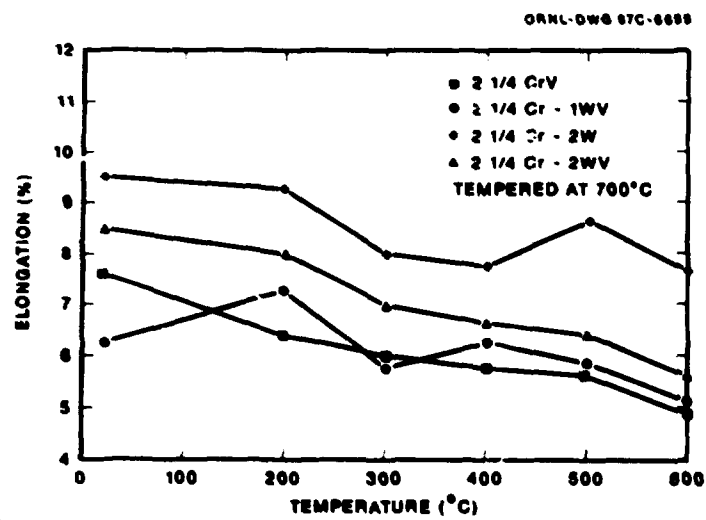
^aAll steels were austenitized for 0.5 h at 1050°C.



(a)

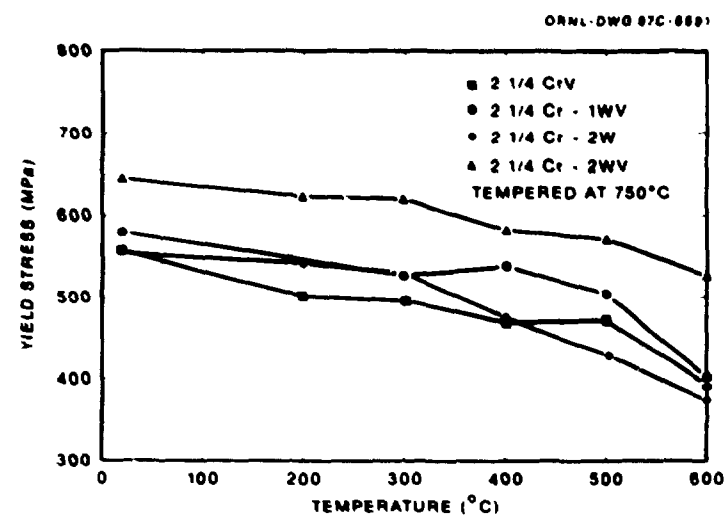


(b)

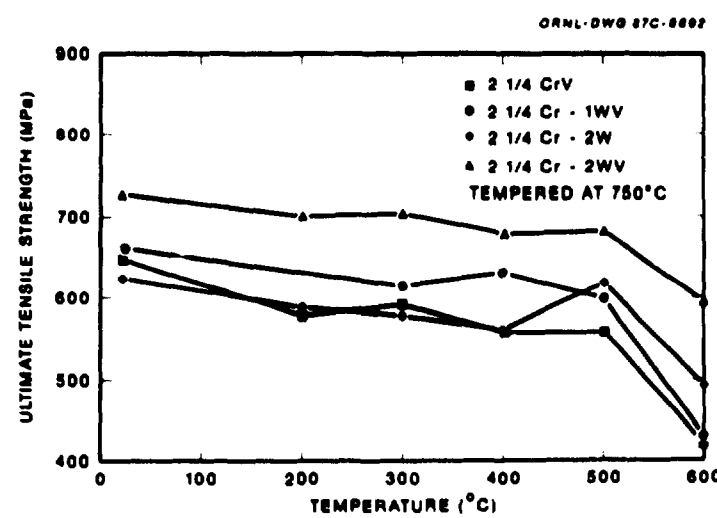


(c)

Fig. 23. Tensile properties as a function of temperature for the 2.25Cr steels tempered at 700°C: (a) 0.2% yield stress, (b) ultimate tensile strength, and (c) total elongation.

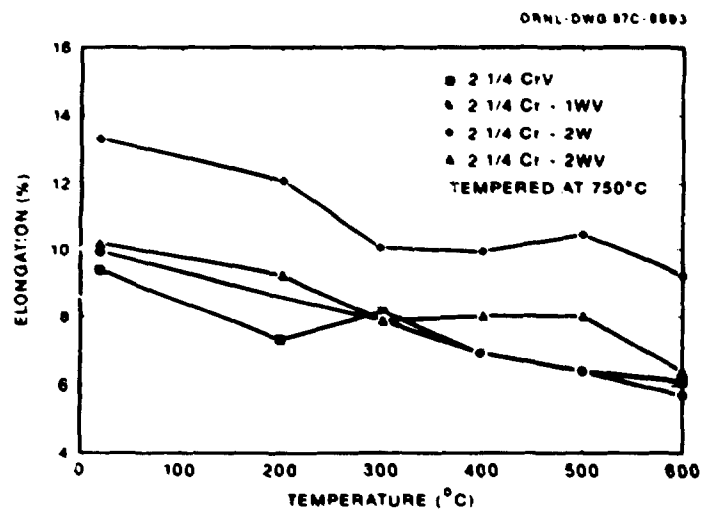


(a)



(b)

4

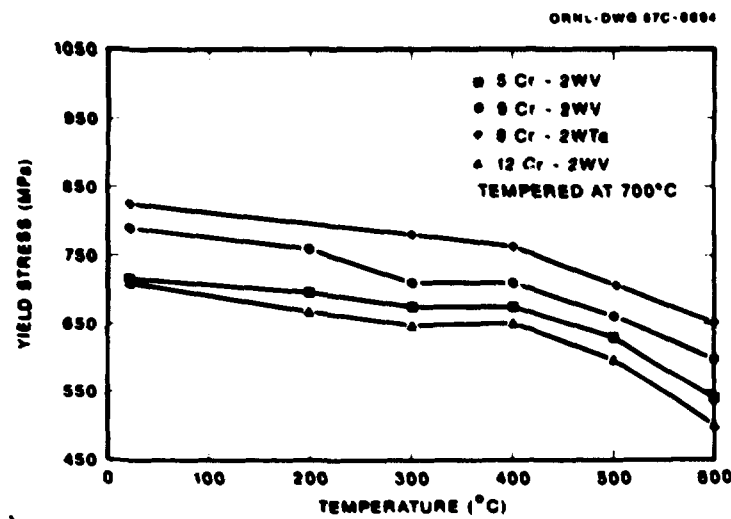


(c)

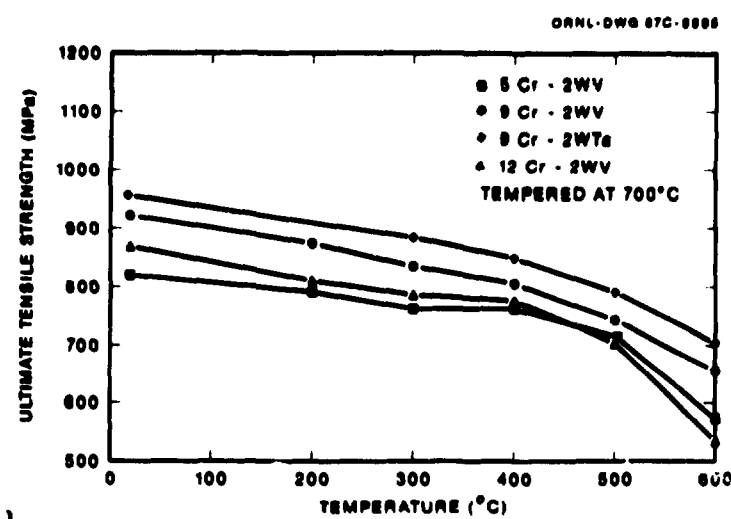
Fig. 24. Tensile properties as a function of temperature for the 2.25Cr steels tempered at 750°C: (a) 0.2% yield stress, (b) ultimate tensile strength, and (c) total elongation.

For the low-chromium steels, an effect of vanadium and tungsten was observed (Figs. 23 and 24). After tempering at 700°C, the effect of vanadium on the 0.2% yield stress (YS) and ultimate tensile strength (UTS) was evident [(Figs. 23(a) and 23(b))]. Except for the UTS at the highest test temperature (600°C), the 2.25CrV steel was stronger than the 2.25Cr-2W steel. The vanadium effect was evident when the 2.25Cr-2W steel was compared to the 2.25Cr-2WV steel. An effect of tungsten in the presence of vanadium was also evident for these test conditions: the 2.25Cr-2WV steel was substantially stronger than the 2.25Cr-1WV steel, which was, in turn, stronger than the 2.25CrV steel. A somewhat similar relationship applied to these steels after tempering at 750°C [Figs. 24(a) and 24(b)], although the difference in the strengths of the 2.25CrV, 2.25Cr-2W, and 2.25Cr-1WV steels was much smaller. Even after tempering at 750°C, however, the 2.25Cr-2WV steel remained substantially stronger than the other steels. Total elongation results [Figs. 23(c) and 24(c)] demonstrated a favorable effect of tungsten on ductility. The 2.25Cr-2W steel, which was often the weakest, had the highest elongation for all test conditions. However, the 2.25Cr-2WV steel, which was always the strongest, had a total elongation that was as great as or greater than the values for the weaker 2.25CrV and 2.25Cr-1WV steels.

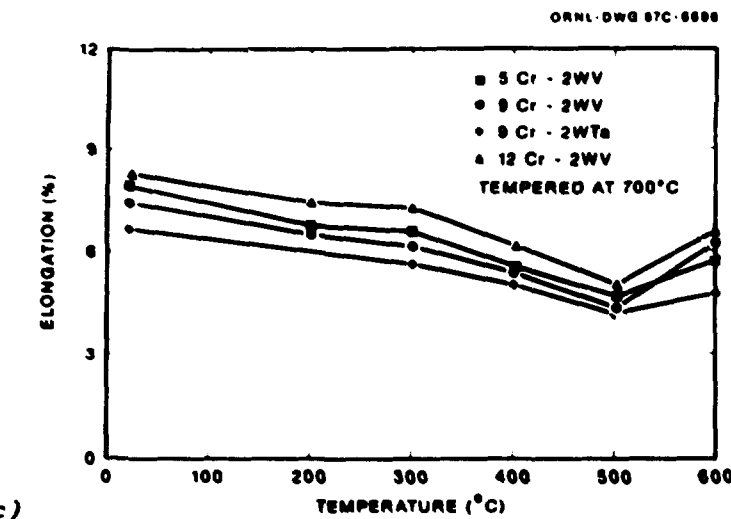
A comparison of the strength behavior for the high-chromium steels (5 to 12% Cr) demonstrated that the 9Cr steels were superior [Figs. 25(a), 25(b), 26(a), and 26(b)]. The small tantalum addition to the 9Cr-2WV steel gave the 9Cr-2WVTa steel the best YS and UTS behavior. The only exception was for the steel tempered at 750°C, where the UTS of the 9Cr-2WV steel was similar to that of the 9Cr-2WVTa steel for the 500 and 600°C tests. From the tempering curves (Figs. 18-20), the 5Cr-2WV steel was expected to be one of the strongest steels. It turned out to be the weakest steel for most conditions. Based on the tempering curves and the large amount of delta-ferrite in the microstructure (Fig. 2), the 12Cr-2WV steel was expected to be among the weakest. This was the case when the steel was tempered at 700°C. It had somewhat better relative strength



(a)

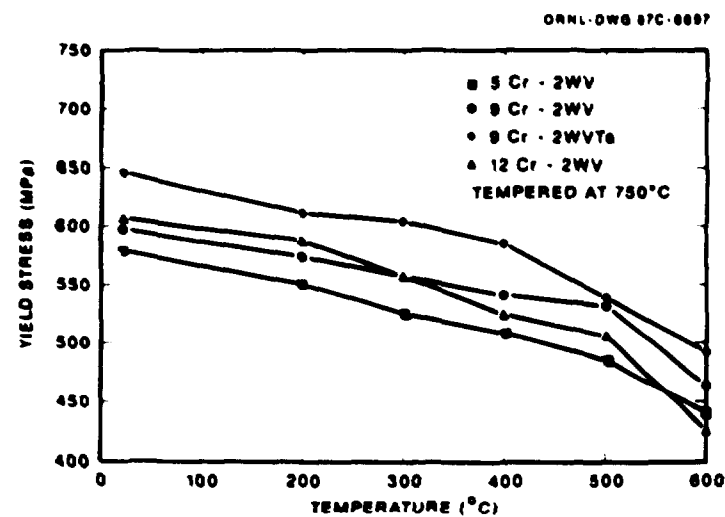


(b)

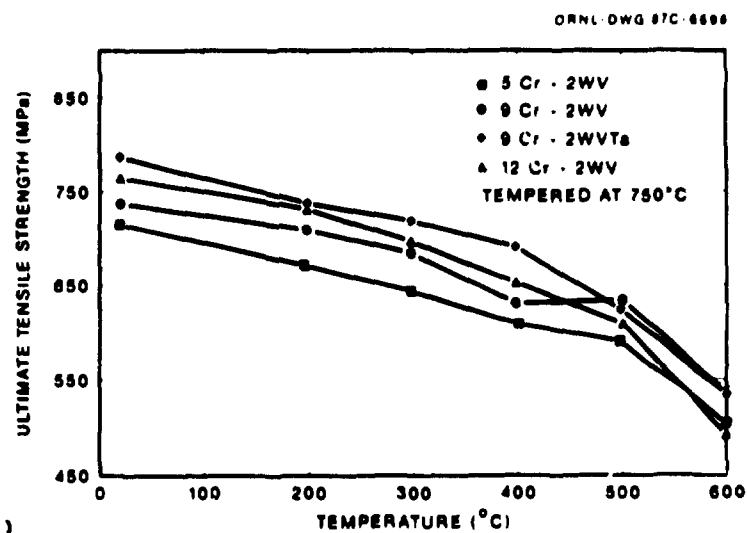


(c)

Fig. 25. Tensile properties as a function of temperature for the 5, 9, and 12Cr steels tempered at 700°C: (a) 0.2% yield stress, (b) ultimate tensile strength, and (c) total elongation.

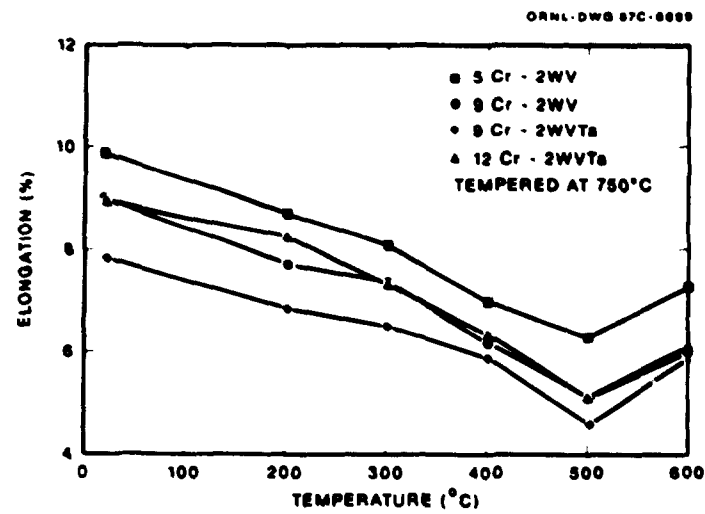


(a)



(b)

67



(c)

Fig. 26. Tensile properties as a function of temperature for the 5, 9, and 12Cr steels tempered at 750°C: (a) 0.2% yield stress, (b) ultimate tensile strength, and (c) total elongation.

when tempered at 750°C, although the strength deteriorated substantially at the highest test temperature [Figs. 25(b) and 26(b)], where it was again the weakest.

Ductilities for the high-chromium steels reflected the inverse of the strength behavior, with the strongest material having the lowest total elongation [Figs. 25(c) and 26(c)].

To compare the behavior of the strongest steels, Figs. 27 and 28 show the properties of the 2.25Cr-2WV, 9Cr-2WV, and 9Cr-2WVTa steels after tempering at 700 and 750°C, respectively. Under most test conditions, the 2.25Cr-2WV steel not only had the best strength properties, but also the best ductility. The only exception in strength was the UTS behavior after the 750°C tempering treatment. In this case, the 9Cr-2WVTa steel was the strongest up to a test temperature of 400°C, but at higher temperatures the 2.25Cr-2WV was again strongest. The only instance where the 2.25Cr-2WV steel did not have the highest ductility occurred when the steel was tempered at 700°C and tested at 600°C. Here the 9Cr-2WV steel had a slightly greater total elongation.

The tensile properties of the 2.25Cr steels tempered at 700°C were compared with 2.25Cr-1Mo steel tempered at 700°C after being normalized exactly the same way as the 2.25Cr-2W (Fig. 29). The YS [Fig. 29(a)] and total elongation [Fig. 29(c)] of the 2.25Cr-1Mo steel were similar to those of the 2.25Cr-2W steel, which is consistent with the initial reason for replacing molybdenum with tungsten. However, the UTS of the 2.25Cr-1Mo was somewhat larger than that for the 2.25Cr-2W steel. In all cases, the strength of the 2.25Cr-2WV steel was substantially better than the strength of 2.25Cr-1Mo steel.

In Fig. 30, the properties of 2.25Cr-2WV and 9Cr-2WVTa—the two strongest heats of FIRD steel—are compared with the 9Cr-1MoVNb and 12Cr-1MoVW steels, the strongest conventional Cr-Mo steels presently being investigated in the fusion reactor materials program. All steels were tempered at 750°C. The reduced-activation Cr-W steels compared favorably with 9Cr-1MoVNb and 12Cr-1MoVW steels. Although the room-temperature UTS values for the Cr-Mo steels were slightly greater than those for the

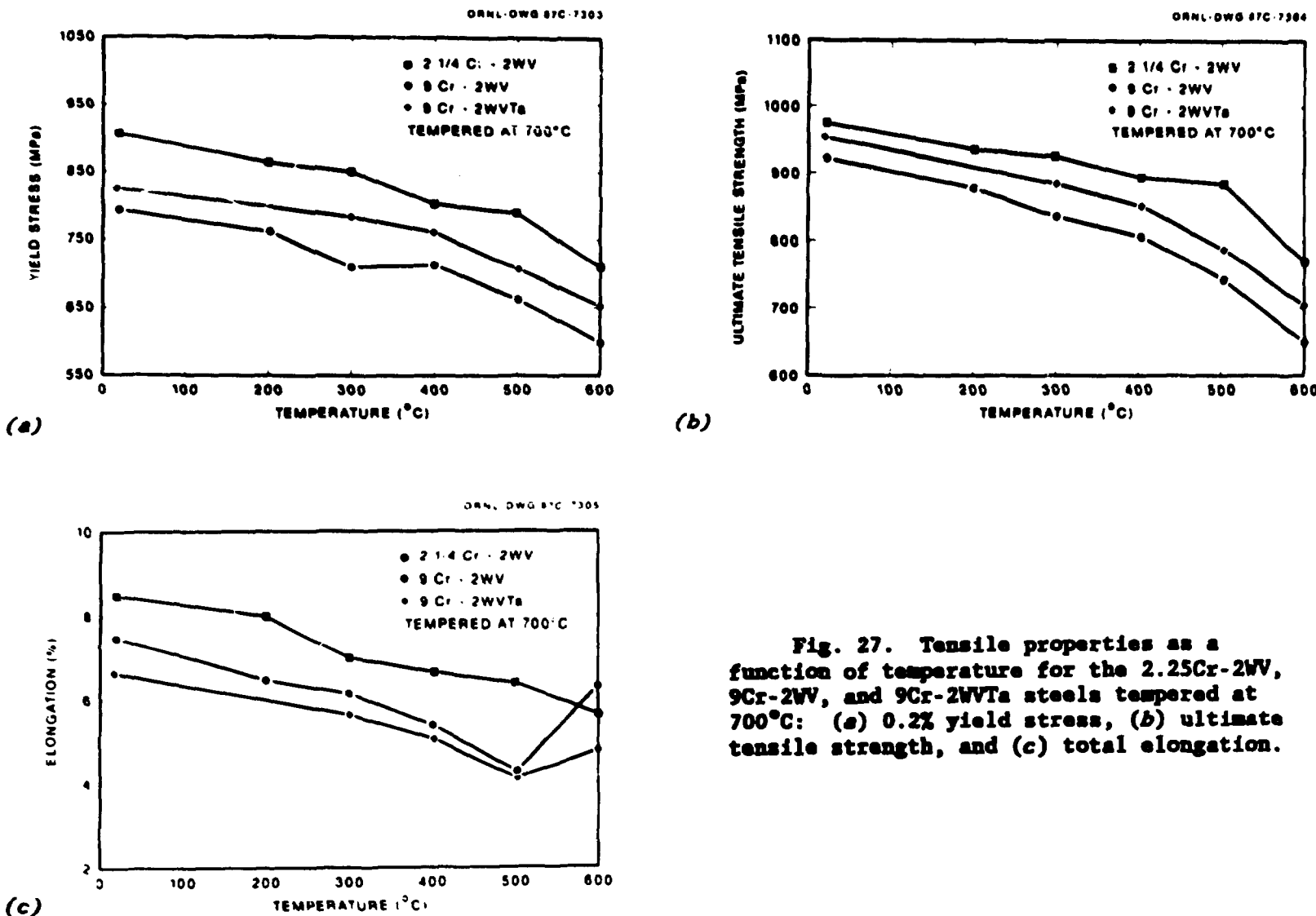


Fig. 27. Tensile properties as a function of temperature for the 2.25Cr-2WV, 9Cr-2WV, and 9Cr-2WVTa steels tempered at 700°C: (a) 0.2% yield stress, (b) ultimate tensile strength, and (c) total elongation.

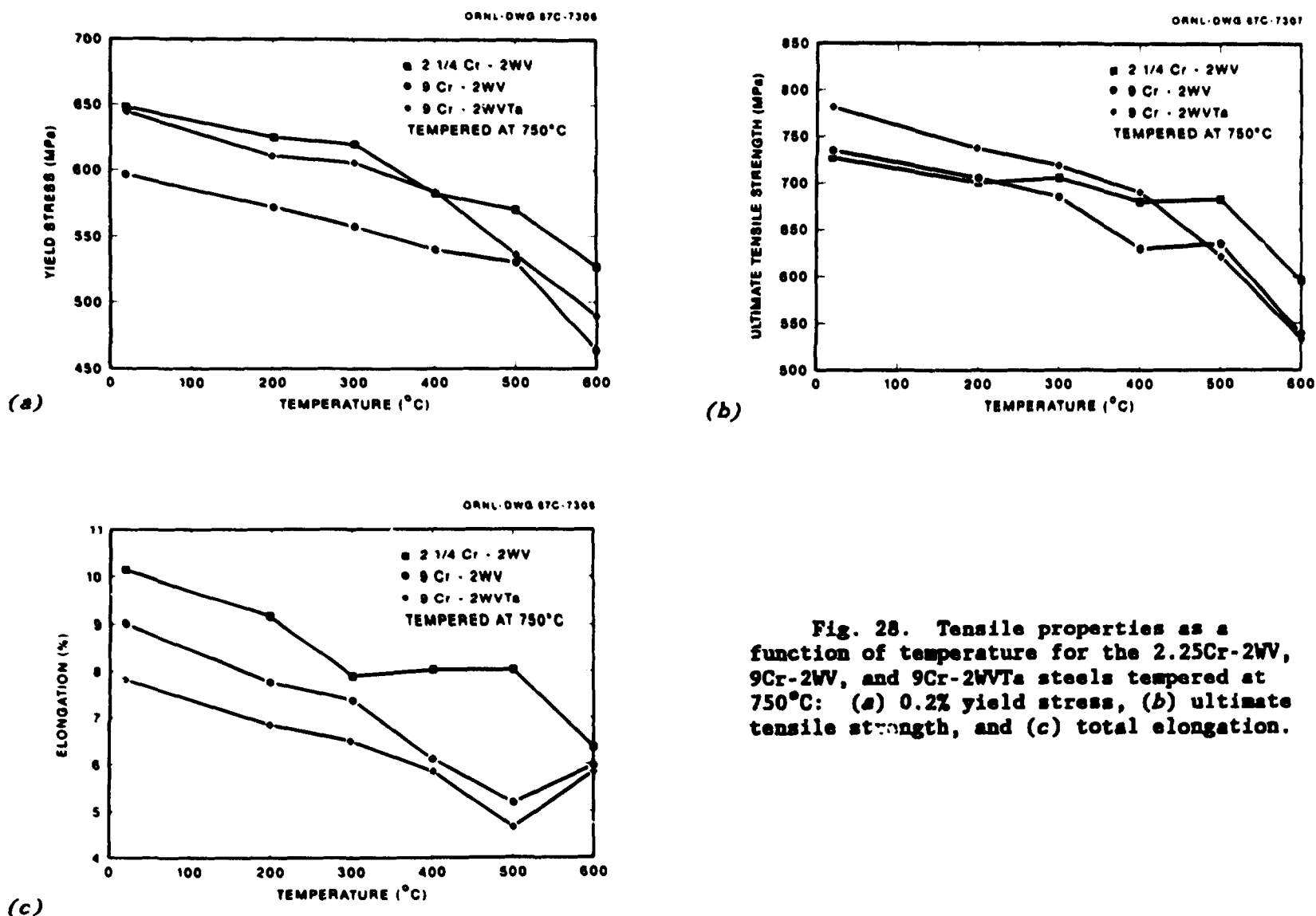


Fig. 28. Tensile properties as a function of temperature for the 2.25Cr-2WV, 9Cr-2WV, and 9Cr-2WVTA steels tempered at 750°C: (a) 0.2% yield stress, (b) ultimate tensile strength, and (c) total elongation.

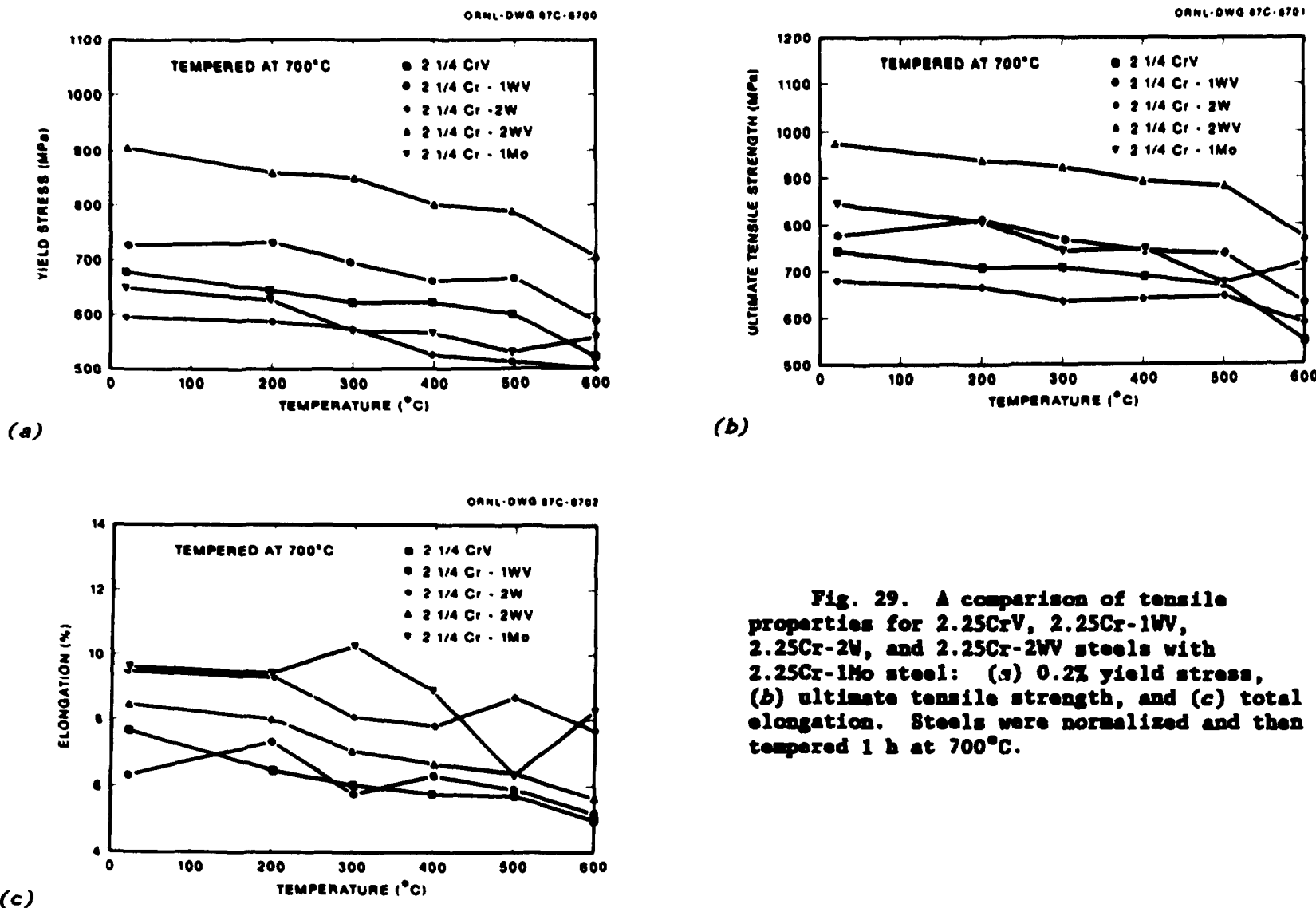
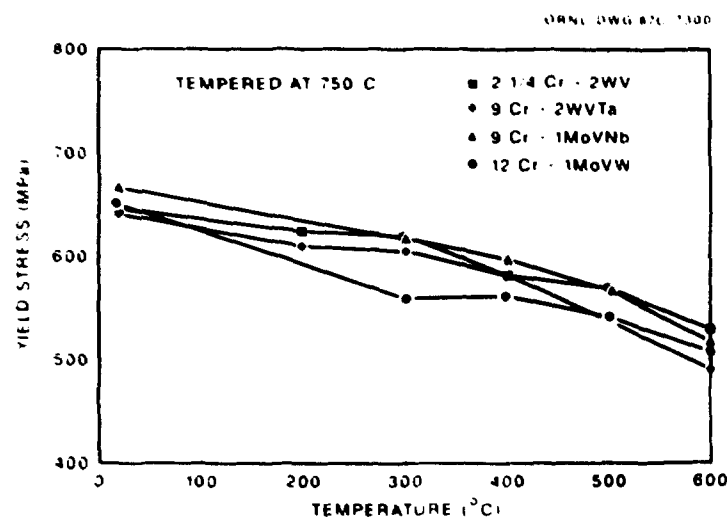
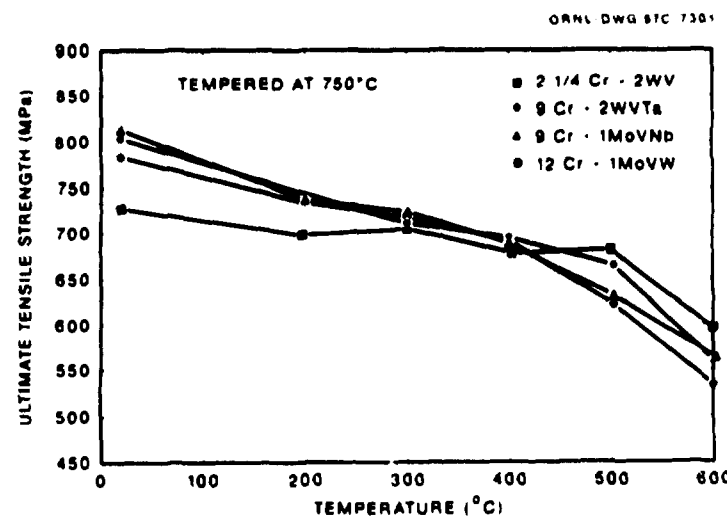


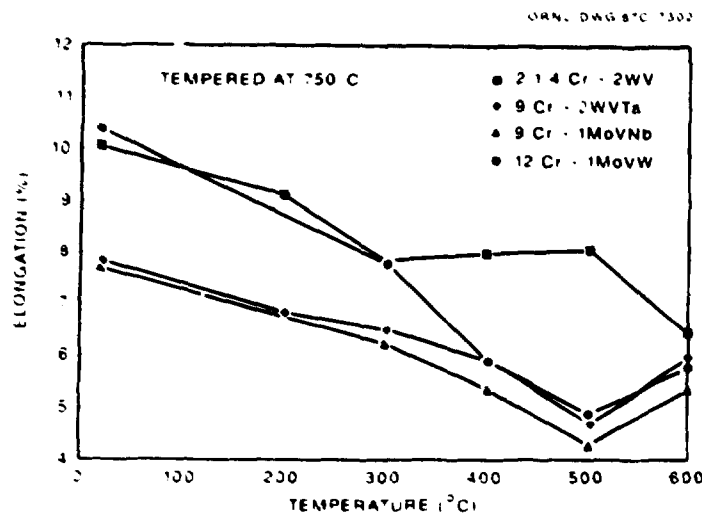
Fig. 29. A comparison of tensile properties for 2.25CrV, 2.25Cr-1WV, 2.25Cr-2W, and 2.25Cr-2WV steels with 2.25Cr-1Mo steel: (a) 0.2% yield stress, (b) ultimate tensile strength, and (c) total elongation. Steels were normalized and then tempered 1 h at 700°C.



(a)



(b)



(c)

Fig. 30. A comparison of the tensile properties for 2.25Cr-2WV, 9Cr-2WV, and 5Cr-2WVTa steels—the strongest Cr-W steels—with the properties for 9Cr-1MoVNb and 12Cr-1MoVW steels: (a) 0.2% yield stress, (b) ultimate tensile strength, and (c) total elongation. Steels were normalized and then tempered for 1 h at 750°C.

2.25Cr-2WV steel, at the elevated temperatures the strengths (YS and UTS) of the 2.25Cr-2WV and the 9Cr-2WVTa steels were similar to the strengths of the Cr-Mo steels.

In general, the ductility of the Cr-W steels as measured by total elongation exceeded that of the two Cr-Mo steels [Fig. 30(c)]. The 9Cr-1MoVNb steel had the lowest total elongation at all test temperatures. By contrast the 12Cr-1MoVW steel had the highest total elongation at room temperature, but then it decreased to values as low or lower than most of the Cr-W steels at higher temperatures. The 2.25Cr-2WV steel had the highest total elongation at all temperatures above room temperature.

IMPACT PROPERTIES

Charpy V-notch impact specimens were machined from the normalized-and-tempered 15.9-mm-thick plates with the microstructures shown in Fig. 1. That means that all of the 2.25Cr steels except the 2.25Cr-2W contained polygonal ferrite, and the 12Cr-2WV steel contained 25% delta ferrite. Tests were made after tempering at 700 and 750°C, with the exception of the 2.25Cr-1WV steel, which was tempered at 725 and 750°C. A summary of the data is given in Table 6, where the ductile-brittle transition temperature (DBTT) and the upper-shelf energy (USE) are given for each steel. A DBTT was determined at the 41- and 68-J level and from lateral-expansion measurements.

Impact curves are shown in Fig. 31 for the 2.25Cr steels tempered at 750°C. The 2.25Cr-2W steel had the lowest DBTT and highest USE. For the vanadium-containing 2.25Cr steels, the 2.25Cr-1WV, and 2.25Cr-2WV steels had similar DBTTs, and they were lower than the DBTT of the 2.25CrV steel. Data scatter was quite large for the 2.25Cr-1WV steel, and the one high point away from the trend of the other data points caused this curve fit to have a lower DBTT than would have been the case if this point had not been included. The 2.25Cr-2WV steel had a lower USE than the other two vanadium-containing steels, which had USE values similar to that of the 2.25Cr-2W steel. When tempered at 700°C (Table 6), the 2.25Cr-2W steel again had the best combination of DBTT and USE. The 2.25Cr-2WV steel had

Table 6. Impact properties of fast induced-radioactivity decay steels

Steel	Tempering temperature ^b (°C)	Impact properties ^a			
		TT _{41J} (°C)	TT _{68J} (°C)	TT _{LE} (°C)	USE (J)
2.25CrV	700	85	86	85	240
	750	66	69	70	318
2.25Cr-1WV	725	52	53	52	220
	750	8	23	38	340
2.25Cr-2W	700	24	24	12	260
	750	-41	-30	-31	324
2.25Cr-2WV	700	85	110	112	131
	750	31	31	31	265
5Cr-2WV	700	-61	-46	-46	219
	750	-97	-76	-83	259
9Cr-2WV	700	7	26	33	157
	750	-69	-49	-42	217
9Cr-2WVTa	700	-47	-24	-20	181
	750	-95	-78	-82	258
12Cr-2WV	700	11	20	19	168
	750	-13	-2	-24	193
9Cr-1MoVNb	700	56	68	68	161
	750	27	41	41	199
12Cr-1MoVW	700	33	68	64	99
	750	4	29	26	115

^aTT_{41J} is 41-J (30 ft-lb) transition temperature; TT_{68J} is 68-J (50 ft-lb) transition temperature; TT_{LE} is lateral expansion transition temperature as determined by 0.889-mm expansion; USE is upper-shelf energy.

^bAll steels were tempered for 1 h; before tempering all steels but the 2.25Cr-2W were normalized at 1050°C; the 2.25Cr-2W was normalized at 900°C.

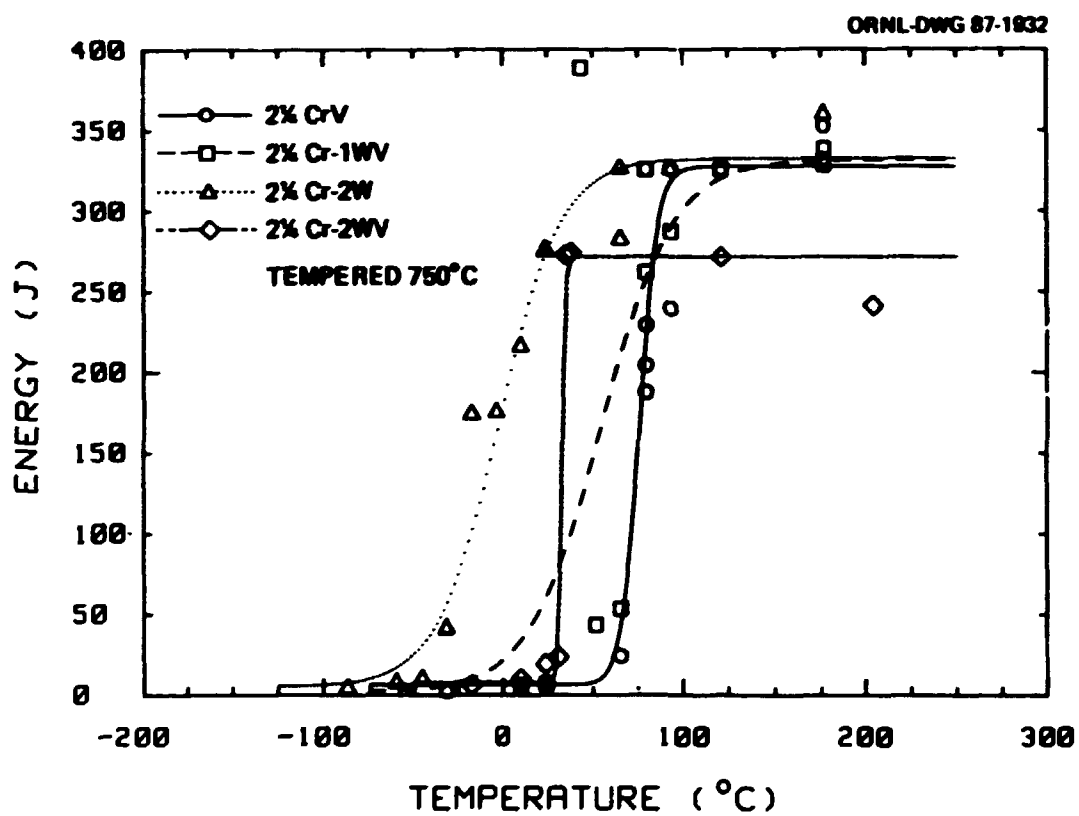


Fig. 31. The Charpy V-notch impact curves for 2.25CrV, 2.25Cr-1WV, 2.25Cr-2W, and 2.25Cr-2WV steels; all steels were tempered 1 h at 750°C.

the worst properties for these tempering conditions. However, the DBTT values of all four steels were considerably above those obtained after tempering at 750°C.

In Fig. 32, the impact curves are shown for the high-chromium steels tempered at 750°C. All of the steels had DBTT values well below room temperature. The superior properties of the 5Cr-2WV and 9Cr-2WVTa are seen; these two steels had similar properties. The 9Cr-2WV steel also had good properties after the 750°C temper. Although the 12Cr-2WV steel contained 25% delta-ferrite, it also had a quite low DBTT and a reasonably high USE. After tempering at 700°C, the relative behavior of the properties of the different steels remained the same (Table 6), but the DBTT is higher and the USE lower than after tempering at 750°C.

For comparison, Charpy impact tests were conducted on the 9Cr-1MoVNb and 12Cr-1MoVW steels (Table 6). Full-size Charpy specimens were machined from 15.9-mm-thick plates that had been austenitized for 1 h at 1050°C, air cooled, and tempered for 1 h at 700°C and for 1 h at 750°C--the identical procedures used for the Cr-W impact specimens. A tempered martensite microstructure resulted for both of the Cr-Mo steels after these heat treatments.

A comparison of the properties for the Cr-Mo steels and the high-chromium Cr-W steels indicated that the Cr-W steel values were better than those for the Cr-Mo steels (Table 6). In Fig. 33, a comparison is shown after the 750°C temper for the two Cr-Mo steels and their Cr-W analogs--the 9Cr-2WVTa and 12Cr-2WV steels. The 9Cr-2WVTa had the best properties, and, despite containing 25% delta-ferrite, the 12Cr-2WV steel had better properties than those of the 9Cr-1MoVNb and 12Cr-1MoVW steels.

DISCUSSION

OPTICAL MICROSCOPY

The microstructures of the plate specimens varied according to the chemical composition. The 2.25Cr alloys showed the effect of the tungsten on hardenability; the steel without tungsten contained the most polygonal

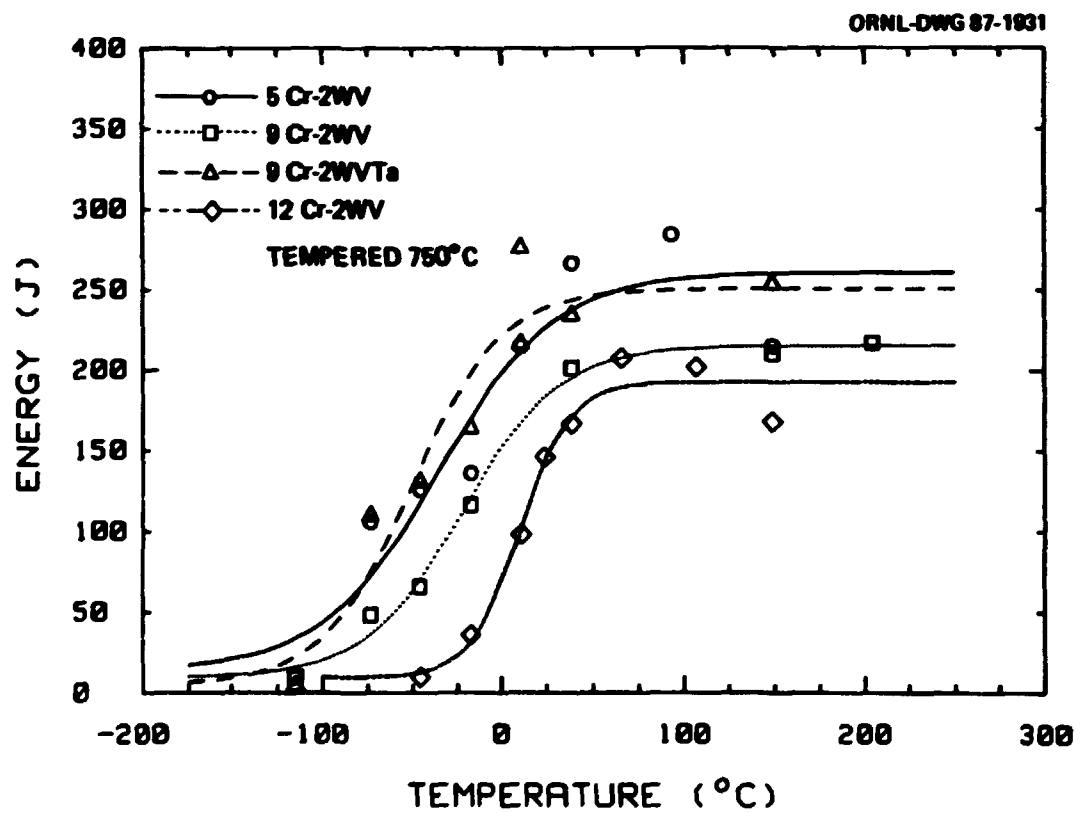


Fig. 32. The Charpy V-notch impact curves for 5Cr-2WV, 9Cr-2WV, 9Cr-2WVta, and 12Cr-2WV steels; all steels were tempered 1 h at 750°C.

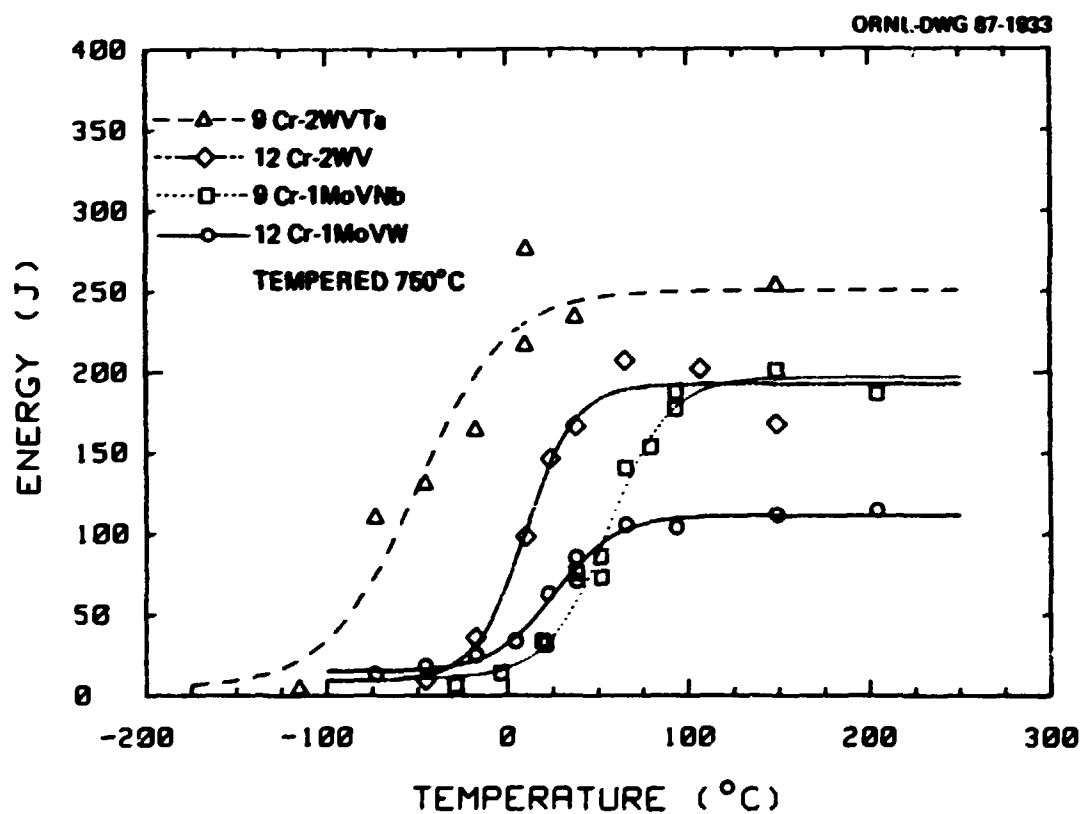


Fig. 33. A comparison of the Charpy V-notch impact curves for 9Cr-2WVTa and 12Cr-2WV steels with the curves for 9Cr-1MoVNb and 12Cr-1MoVW steels; all steels were tempered for 1 h at 750°C.

ferrite, followed by the steel with only 1% W. Since no ferrite was detected in the 2.25Cr-2W steel, the appearance of ferrite in the 2.25Cr-2WV steel was unexpected. One possible explanation is that the vanadium carbide present when the 2.25Cr-2WV steel was austenitized did not completely dissolve. The lower concentration of carbon in solution could then lower the hardenability. This possibility was anticipated, and, therefore, 1050°C was chosen as the austenitization temperature for the 2.25Cr-2WV steel and only 900°C for the 2.25Cr-2W steel. The 1050°C temperature was considered high enough to dissolve the vanadium carbide, and the austenitization tests tended to confirm that conclusion (Fig. 17), because the maximum hardness was reached after austenitization at 1000°C. With the increase in chromium to 5% or more, the hardenability becomes great enough to form martensite instead of bainite.

Although the 12Cr-2WV steel was patterned after the 12Cr-1MoVW steel that is ~100% martensite when normalized, the appearance of 25% delta-ferrite in the microstructure indicated that insufficient amounts of austenite-stabilizing elements were present to completely austenitize the steel. The 12Cr-1MoVW steel contains approximately 0.5% Ni and 0.2% C, both austenite-stabilizing elements, whereas the 12Cr-2WV steel contains approximately 0.1% C and no nickel. Significant amounts of nickel are intentionally omitted in a FIRD steel,³ and the carbon content was restricted to 0.1% to ensure good weldability. As discussed below, a 100% martensitic alloy is again possible if more carbon and manganese are added.

TRANSMISSION ELECTRON MICROSCOPY AND PRECIPITATE IDENTIFICATION

The bainite of the low-chromium steel was of the granular type typical of that in 2.25Cr-1Mo steel that occurs under certain heat-treatment conditions. The martensite of the 9Cr and 12Cr steels was the lath type that is observed in the 9Cr-1MoVNb and 12Cr-1MoVW steels.¹¹

Precipitate morphology observed in the 2.25Cr steels was characteristic of the precipitation that accompanies the austenite-to-polygonal-ferrite transformation in alloy steels. Because the eutectoid composition

in such steels occurs at lower carbon concentrations and higher temperatures than in the Fe-C system, classical pearlite does not appear.¹³ Three different types of ferrite-carbide microstructures are observed: fibrous carbides, interphase precipitates, and carbides that form within the supersaturated ferrite during tempering, often forming on dislocations.¹³ The first two types of precipitation occur at a moving austenite-ferrite interface. Fibrous precipitates are analogous to pearlite and occur at an incoherent phase boundary; they are much closer to equilibrium than the interphase precipitates. Fibers are associated with a high transformation temperature and a slowly moving interface. Interphase precipitates form at lower temperatures at a low-energy interface by the movement of steps along the boundary.¹³

Fibrous and interphase morphologies were present in large quantities in the 2.25CrV and 2.25Cr-1WV steels because they contained large amounts of polygonal ferrite. The large blocky types of precipitate observed in the matrix of these steels occurred in the bainitic regions of the steels. Most of the precipitates in the 2.25Cr-2W steel were of the blocky type, because this steel contained essentially no polygonal ferrite.

Considerable research has been conducted on Fe-V-C alloys in an effort to use the interphase precipitates for dispersion strengthening.¹³ (The effect of the fibrous precipitates on strength is unknown, although the properties are not expected to be as favorable as are those of a fine interphase precipitate.) Steels containing a uniform dispersion of interphase precipitates have been developed that have properties superior to those of tempered martensite.¹⁴ Such a distribution of interphase precipitates is most easily obtained by an isothermal transformation.^{13,14} However, an isothermal heat treatment is generally not practical in commercial practice. Studies have been made to determine how interphase precipitates could be developed during a continuous cool from the austenitizing temperature. One proposal for accomplishing this (and maintain the FIRD characteristics of the steel) is to add manganese to the steel.¹⁴ Considerable research would be required to develop such alloys for commercial production, and at present only continuous cooling of FIRD steels is being investigated.

The observations on fibrous and interphase precipitates in the 2.25CrV and 2.25Cr-1WV steels were consistent with the above discussion. Both the chromium and vanadium carbides were observed to form as fibers, although the chromium-rich fibers were much coarser and appeared ribbon-like. This observation agrees with previous work that showed that chromium carbides form coarser fibers than do vanadium carbides.⁴ The observation that fibers and interphase precipitates form in a finer distribution in the 2.25Cr-1WV can be attributed to the difference in the transformation characteristics for these two steels. Because of the higher hardenability of the steel with tungsten, the transformation in this steel must occur at a lower temperature. A much finer precipitate distribution of all the carbide morphologies was evident in the steel with 1% W. Also, in the 2.25Cr-1WV steel, none of the ribbon structures were evident. Similarly, the small amount of fibrous and interphase precipitate that formed in the 2.25Cr-2WV steel was finer than found in the 2.25Cr-1WV steel.

A synergistic effect of tungsten and vanadium was evident in the microstructures and tensile properties of the 2.25Cr steels. The overall carbide distribution of the 2.25Cr-2W steel was coarser than the carbide distributions in the steels containing vanadium, including the steel without tungsten. The tensile properties reflected this coarser precipitate distribution, because the 2.25Cr-2W steel was generally the weakest or had properties approaching those of the 2.25CrV (Fig. 29).

With the exception of the MC phase, the carbides in the 2.25Cr steels were similar to those observed in 2.25Cr-1Mo steel.¹⁵ The carbides detected by X-ray diffraction— M_3C , M_2C_3 , and M_23C_6 —are also observed in 2.25Cr-1Mo steel; M_2C and M_6C have been observed as well.¹⁵ The carbides present in the 2.25Cr-1Mo steel depend on the heat treatment the steel is given.¹⁵

The precipitates in the 2.25Cr-2W steel were quite similar to those in 2.25Cr-1Mo steel. Although M_2C was not detected by X-ray diffraction in the 2.25Cr-2W steel, TEM confirmed the presence of many fine needles, which would constitute only a small fraction of the total precipitate and could be undetectable above background by X-ray diffraction. XEDS analysis indicated that the needles in the 2.25Cr-2W steel are probably

M_2C (or M_2X). Those needles were chromium and tungsten rich, but contained more chromium than tungsten. The needles that form in 2.25Cr-1Mo steel have been generally concluded to be molybdenum-rich M_2C , containing about 80% Mo and lesser amounts of Fe, Cr, and Si (refs. 15 and 16). However, in other work on 2.25Cr-1Mo steel, the needles have been identified as M_2X , which was chromium rich with relatively large amounts of molybdenum.¹⁷ This is similar to the observations in the present work on the 2.25Cr-2W, with the molybdenum being replaced by tungsten.

For the 9Cr and 12Cr steels, the coarser carbides were primarily M_23C_6 , although TEM detected finer particles that could be identified as MC from XEDS analysis. Similar carbides were found in the 9Cr-1MoVNb and 12Cr-1MoVW steel.^{11,18} The coarse carbides in the 5Cr-2WV steel were a mixture of the chromium-rich carbides found in both the low- and high-chromium steels. Both M_7C_3 and M_23C_6 were observed, indicating how the matrix chromium concentration governs the transition from one type of carbide to another.

The large amount of precipitation that occurred on prior austenite grain boundaries and lath boundaries in the microstructures of the 5Cr, 9Cr, and 12Cr steels was similar to that observed in the 9Cr-1MoVNb steel.¹¹ Much more precipitate was observed in the 12Cr-1MoVW steel,¹¹ but this steel contained 0.2% C, twice as much carbon as the 9Cr-1MoVNb steel, and the steels of the present study.

Compositions of the M_23C_6 precipitates in the 9Cr-2WV and 9Cr-2WVta steels are analogous to those found in 9Cr-1MoVNb steel (Fig. 34).^{11,18} The relative amounts of Cr, Fe, and V are similar; the only difference is that the molybdenum in the 9Cr-1MoVNb is replaced by tungsten.

Finally, it is important to note the compositional behavior of the MC phase in the various alloys (Fig. 35). The fine distribution and small volume fraction of MC particles make their study difficult by bulk extraction and X-ray diffraction techniques, but they are easily studied with modern microanalytical techniques. Two types of MC were observed in the 9Cr-2WVta steel: one was vanadium rich and similar to that found in the 9Cr-2WV [Fig. 35(b)], while the second was tantalum rich [Fig. 35(c)].

ORNL DWG 8/ 13202

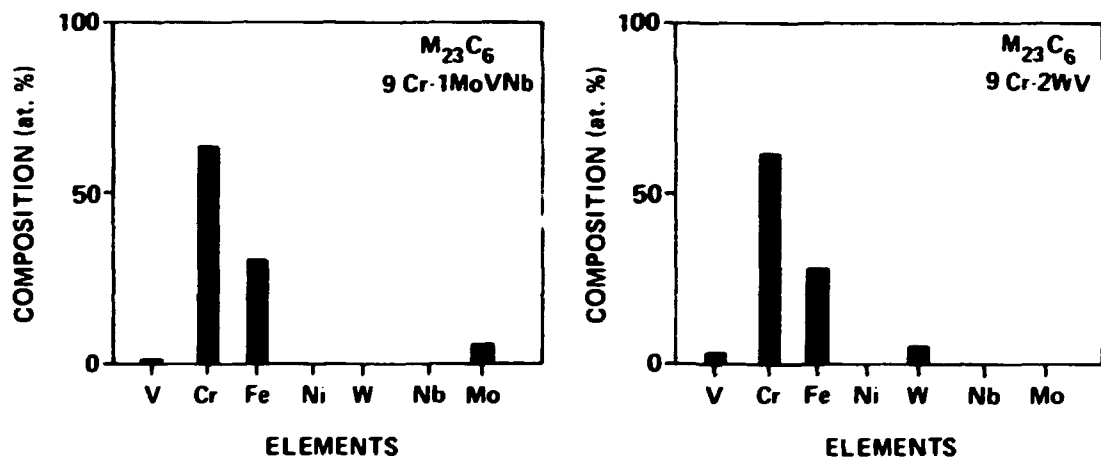


Fig. 34. A comparison of the phase compositions for $M_{23}C_6$ in (a) 9Cr-1MoVNb and (b) 9Cr-2WV steels as determined on extraction replicas by XEDS; the $M_{23}C_6$ in the 9Cr-2WVta steel was similar.

ORNL-DWG 87-13201

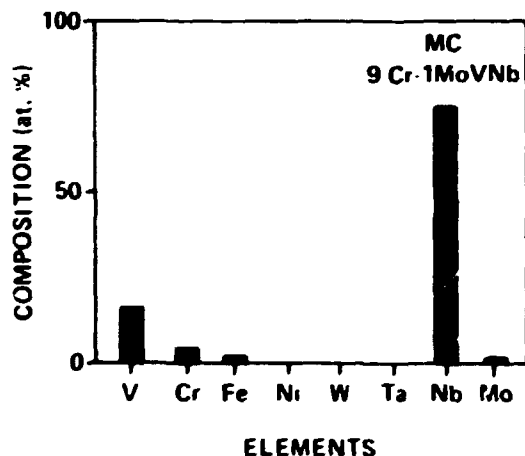
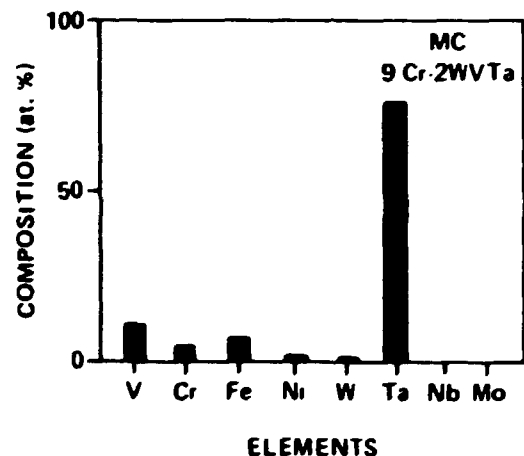
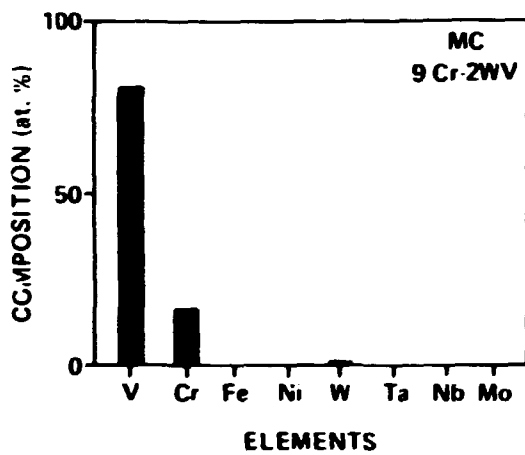
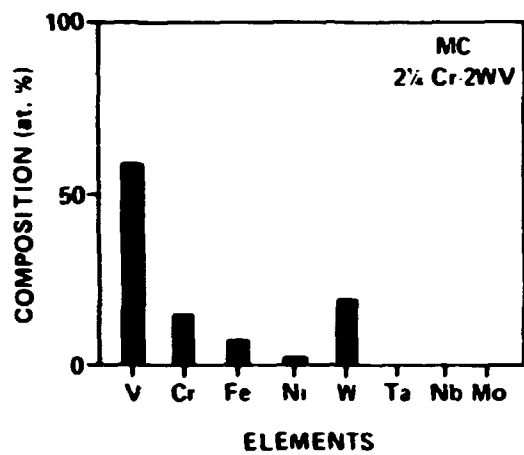


Fig. 35. The compositions of the MC phase as determined on extraction replicas by XEDS in (a) 2.25Cr-2WV, (b) 9Cr-2WV, (c) 9Cr-2WVTa, and (d) 9Cr-1MoVNb steels.

A similar dual precipitate composition was observed for the 9Cr-1MoVNb, where vanadium-rich and niobium-rich carbides were observed [Fig. 35(d)]. From a comparison of Figs. 35(c) and 35(d), it can be seen that the tantalum-rich and niobium-rich carbides are analogous with the interchange of tantalum and niobium.

The data in Fig. 35(a) reveal an important synergistic effect between vanadium and tungsten in forming the fine MC needle carbides in the 2.25Cr alloys that is not observed for the higher chromium steels containing vanadium and tungsten. Tungsten is enriched only in the MC formed in the 2.25Cr-2WV steels. It also suggests an important difference between tungsten and molybdenum that is influenced by the chromium content of the alloy. Molybdenum is never found to concentrate significantly in the vanadium-rich MC formed in various martensitic steels.^{11,18} The synergism between vanadium and tungsten is also unique relative to the other MC-forming elements. In most cases, there is not as much solubility of vanadium in MC carbides that are rich in niobium or tantalum (Fig. 35). The formation of a mixed vanadium-tungsten MC carbide may be a key to the fine and uniform distribution of needles that results in the superior strength of the 2.25Cr-2WV steel.

HEAT TREATMENT STUDIES

Austenitizing Studies

Results from the austenitization studies on 0.76-mm-thick sheet showed that tungsten plays an important role in the hardening of these steels, since the steels with 2% W were considerably harder than the steels with 0 and 1% W (Fig. 17). Vanadium had little effect on the normalized hardness. The relative hardnesses of the normalized steels also demonstrated the difference between untempered bainite and untempered martensite. The 5Cr and 9Cr steels were expected to be entirely martensite, and the 2.25Cr steels, when heat treated in the sheet form, were entirely bainite. As seen in Fig. 17, the hardness of the martensite does not depend on the chromium content. The 12Cr steel with a duplex martensite and delta-ferrite microstructure had a maximum hardness that

fell between that of the martensitic and bainitic steels. The difference between the 9Cr and 12Cr steels can be attributed to the delta-ferrite in the 12Cr steel. The low hardness value after the 900°C austenitization for the 12Cr-2WV is an indication that larger amounts of ferrite were present in this steel after austenitizing at 900°C than after the higher temperature anneals.

From Fig. 17, it appears that for the thin sheet specimens it is not necessary to austenitize at the highest temperature (1050°C) to achieve the maximum hardness. Only the 2.25CrV steel developed its maximum hardness at 1050°C. All of the other steels approached the maximum hardness at 1000°C and, in many cases, at 950°C. The steel without vanadium (2.25Cr-2W) reached its maximum hardness with the 900°C anneal. The hardness decrease for this steel when austenitized at higher temperatures could be caused by the increased austenite grain size that results at higher austenitization temperatures for a steel without a strong carbide former (e.g., vanadium).

Tempering Studies

Although vanadium carbide is expected to play an important role in the strengthening of these steels, for the 2.25Cr steels there was apparently a synergistic effect from the tungsten and vanadium. The hardness of the 2.25Cr-2WV steel exceeded that for the 2.25Cr-1WV steel, and both of these steels exceeded the hardness of the 2.25Cr-2W after tempering at 650°C and above. The greater hardness of the 2.25Cr-2W steel after normalizing and after tempering at 600°C was probably because this steel is entirely bainitic, whereas the 2.25Cr-1WV steel contained significant amounts of polygonal ferrite. Early precipitation of abundant M_2C or M_2X may also have played a role in the 2.25Cr-2W steel's achieving its greater hardness at the lower tempering temperatures. At the higher tempering temperatures, the presence of MC in the vanadium-containing steels with tungsten presumably caused these steels to have the higher hardness values. The fact that the 2.25CrV and 2.25Cr-2W steels have similar hardnesses at 650°C and above is an indication that neither the vanadium nor tungsten alone provides the tempering resistance. Likewise, this

shows that the 100% bainitic structure is not inherently the strongest (the 2.25Cr-2W steel was the only steel with a 100% bainitic microstructure).

Because of the high hardenability of steels with 9 and 12% Cr, such steels are expected to transform from austenite to martensite when normalized (the delta-ferrite in the 12Cr steel does not transform). For the low-chromium steels, the lower hardenability makes an entirely martensitic or bainitic structure difficult to obtain. Furthermore, it is often difficult to differentiate between martensite and bainite. The hardness of martensite in such steels depends almost entirely on the carbon content, and for a steel with approximately 0.1% C, the R_C hardness of martensite is expected to be about 38 (ref. 12). This is very close to the hardness of the normalized 5Cr and 9Cr steels, which were concluded to be 100% martensitic.

The acicular-appearing constituent in the 2.25Cr steels (Fig. 1) was assumed to be bainite, which agrees with the normalized hardness. This microstructure was also expected from observations on 2.25Cr-1Mo steel, since it was expected that the hardenability of the 2.25Cr-2W steel should be similar to 2.25Cr-1Mo steel. Extremely rapid cooling rates after austenitizing (e.g., a water quench or the air cooling of a thin section) are required to produce martensite in steels with smaller amounts of alloying elements.

The 2.25Cr-1WV and 2.25Cr-2WV steels were more resistant to tempering than 2.25Cr-1Mo steel (Fig. 19), probably because they contained vanadium. Tempering resistance for the 2.25Cr-2W steel was comparable to that of 2.25Cr-1Mo steel. Since the 2.25Cr-2W steel was taken as analogous to 2.25Cr-1Mo steel, the equivalent tempering response indicates that, on an atom-for-atom basis, molybdenum and tungsten play similar roles in these steels—which was the objective in replacing the molybdenum with tungsten.

The tempering studies indicated that for long tempering times or high tempering temperatures, the 2.25Cr-2WV, 5Cr-2WV, 9Cr-2WV, 9Cr-2WVTa, and 12Cr-2WV steels behaved similarly. This occurred despite the fact that the 2.25Cr-2WV steel was bainitic with 15-20% polygonal ferrite and the high-chromium steels were entirely martensitic. Furthermore, the 12Cr-2WV steel, which contained 25% delta-ferrite and was much softer than the

other martensitic steels after the normalizing and low-temperature tempering treatments, developed hardnesses similar to the other martensitic steels after longer tempering times or higher tempering temperatures. The excellent tempering behavior of these five Cr-W steels along with the favorable comparisons to the tempering behavior of the Cr-Mo steels points to a range of compositions that may be available for the FIRD steels.

ELIMINATION OF DELTA-FERRITE FROM 12Cr-2WV STEEL

It was possible to eliminate much of the delta-ferrite from the 12Cr-2WV by adding manganese and carbon. When tempered, the two steels with manganese added showed the effect of manganese on lowering the A_{C1} temperature. Because of the lower A_{C1} temperature, austenite formed during tempering at the higher temperatures, and when the specimen was cooled from the tempering temperature, martensite formed. A minimum in the tempering curves occurred because the formation of increasing amounts of untempered martensite with increasing tempering temperature caused the hardness to increase with tempering temperature. With 5.6% Mn, the A_{C1} temperature was between 650 and 700°C, and, with 2.8% Mn, it was between 750 and 780°C (Fig. 22). Thus, a high-manganese steel would require a maximum tempering temperature below 700°C to avoid a microstructure that contained untempered martensite.

If all of the modified steels were tempered at temperatures below the A_{C1} of the 5.6% Mn steel, the 0.2% C steel would probably show the best tempering resistance. However, when the 0.2% C steel was compared to the base composition (0.1% C) after tempering at 700°C, little difference in hardness was observed between these two steels or with the steel containing 2.8% Mn (Fig. 22). Furthermore, the duplex steel with 25% delta ferrite had hardness values (after long tempering times or high tempering temperatures) similar to the values for the martensitic steels with 5 and 9% Cr. Thus, it might be possible to consider a duplex steel for a fusion reactor first wall. Because of its better welding

characteristics, a 9Cr-2Mo duplex steel is being considered as a first-wall candidate for the Japanese fusion program.¹⁹ However, a problem with such steels is that the presence of delta-ferrite is believed to cause an increase in DBTT. This will be discussed in a later section. Finally, there is concern that ferrite will not be as radiation resistant (swelling resistant) as bainite or martensite. Definitive studies have yet to be done on this question.

Although the results of adding manganese and carbon to the base composition of the 12Cr-2WV steel demonstrated that it is possible to eliminate much of the delta-ferrite, there are other considerations that must be taken into account. If lithium is to be used as the coolant for the first wall of a fusion reactor, the manganese concentration would have to be minimized, since manganese is highly soluble in lithium. It may therefore be preferable to use 0.2% C plus the minimum manganese required to retard delta-ferrite formation (probably about 1.5% in the presence of 0.2% C).

TENSILE PROPERTIES

The tensile properties of the 2.25Cr steels were affected by the combination of tungsten and vanadium. The steel with 0.25% V and no tungsten had strength properties similar to the steel with 2% W and no vanadium. The steel with 2% W had excellent ductility. With the combination of tungsten and vanadium, an additive effect occurred to give a steel with excellent strength and ductility.

When the tensile data for the steels with 2.25%, 5%, and 9% chromium with 0.25% V and 2% W were compared, it appeared that the chromium had a nonlinear effect on the strength. The strength went through a minimum between 2.25% Cr and 9% Cr, making the 5Cr-2WV steel weaker than either the 2.25Cr-2WV or the 9Cr-2WV steels. A minimum in strength near 5% Cr has also been observed for Cr-Mo steels with chromium compositions between 2.25 and 9%.²⁰ This minimum must be associated with the difference in precipitates that formed in the 5Cr steel. The chromium-rich carbides were different in these steels—the 5Cr steel contained a mixture of M_7C_3 and M_23C_6 , whereas the 2.25Cr steel contained M_7C_3 and the 9Cr steel

contained $M_{23}C_6$. In addition, a much finer distribution of vanadium-rich MC seemed to form in the 2.25Cr-2WV and the 9Cr-2WV steels than in the 5Cr-2WV steel.

Except for the YS of the steels tempered at 700°C, the strength of the 5Cr-2WV steel was less than that for 12Cr-2WV, which contained 2% delta ferrite. The large delta-ferrite content resulted in the lower strength for this latter steel. Tensile results for the high-chromium steels (Figs. 25 and 26) demonstrated the benefit of the addition of tantalum to the 9Cr-2WV steel. Just as niobium improves the strength in the 9Cr-1MoVNb steel, tantalum can be used to improve the strength of a Cr-W steel.

The observation that the 2.25Cr-2WV steel generally had the highest strength of the eight steels investigated was not totally unexpected, if we accept the assumption that 2% W will play the same role as 1% Mo does in the Cr-Mo steels. It is known that the major effect of chromium above 2.25% is to increase the hardenability and corrosion resistance.²¹ Such observations of equivalent strength are made when appropriate micro-structures are compared (i.e., tempered bainite in the 2.25Cr steel is compared to tempered martensite in the high-chromium steel).²¹ Such results would not be expected if the 2.25Cr steel contained large amounts of polygonal ferrite.

The high strength of the 2.25Cr-2WV steel must be the result of the fine MC that formed in this alloy. A unique feature of that precipitate was that it was both vanadium and tungsten rich. This contrasted with the MC in the other Cr-W alloys and for some of the large particles in the 2.25Cr-2WV; these MC particles were mainly vanadium and chromium rich. An exception to this was the 9Cr-2WVta steel, where a tantalum-rich MC was present, in addition to the vanadium-rich MC. It should be noted that the tensile properties of the 2.25Cr-2WV steel were not affected by polygonal ferrite, since the tensile specimens were taken from 0.76-mm sheet that was entirely bainite.

The strength of 9Cr-1MoVNb and 12Cr-1MoVW steels have often been compared to the strength of 2.25Cr-1Mo steel and found superior.²² However, such a comparison ignores the presence of the strong carbide-forming elements like vanadium and niobium in 9Cr-1MoVNb and 12Cr-1MoVW

and the important role these elements play in determining the strength. It has been pointed out that the addition of a strong carbide former to 2.25Cr-1Mo steel should also result in improved properties relative to the higher chromium steels.²³ The present results confirm this. The use of a lower chromium ferritic steel for first walls of future fusion reactors has been shown to have advantages.²³ As shown in the present study, not only is the development of such steels possible, they could have a strength similar to the strength of higher-chromium steels. Presumably this would apply to Cr-Mo steels as well as Cr-W steels.

It is not possible to adequately compare the properties of the steels examined in the present work with the reduced-activation steels being developed elsewhere.⁵⁻¹⁰ This is true because different heat treatments are used by the different investigators, not allowing for a common comparison.

The objective in the development of the Cr-W steels was to achieve properties comparable to the Cr-Mo steels presently in the fusion reactor program. This objective would be met for the 2.25Cr steels if the 2.25Cr-2W steel has properties comparable to the analogous 2.25Cr-1Mo steel. This was the case depicted in Fig. 29, showing that the replacement of molybdenum by tungsten can result in steels with comparable tensile properties. An addition of vanadium then results in steels with improved properties over those for 2.25Cr-1Mo steel. Likewise, the 9Cr-2WVTa steel had tensile properties comparable to those for 9Cr-1MoVNb, after which it was patterned (Fig. 30). The strength properties of the 12Cr-2WV steel were not equivalent to those of the 12Cr-1MoVW steel. However, this was caused by the large amount of delta ferrite in the 12Cr-2WV steel microstructure.

These preliminary tests indicated that the 2.25Cr-2WV and 9Cr-2WVTa steels have tensile properties comparable to the strongest Cr-Mo steels in the fusion program—9Cr-1MoVNb and 12Cr-1MoVW steels. With more development work, it should be possible to further improve on the properties. Note also that the 2.25Cr-2W steel has properties similar to those of 2.25Cr-1Mo steel. In commercial practice, the 2.25Cr-1Mo steel is used for elevated-temperature applications up to 550 to 600°C.

IMPACT PROPERTIES

For fusion reactor applications, impact properties are expected to be crucial. When irradiated by neutrons, the DBTT of the 12Cr-1MoVW steel can increase by over 200°C.^{24,25} Therefore, it may be desirable that any steel used for such applications have as low a DBTT as possible in the unirradiated condition.

When the results for the Cr-W steels were compared against the results for 9Cr-1MoVNb and 12Cr-1MoVW steels for similar heat treatments (Table 6), the properties of the 5Cr-2WV, 9Cr-2WV, 9Cr-2WVTA, and 12Cr-2WV steels were superior to those for 9Cr-1MoVNb and 12Cr-1MoVW steels. However, the results in Table 6 for the Cr-Mo steels are not the optimum for these heats of steel.^{25,26} A DBTT of ~-50°C and a USE of -255 J were obtained for the 9Cr-1MoVNb heat when it was austenitized for 1 h at 1038°C and tempered for 1 h at 760°C.²⁵ For the 12Cr-1MoVW heat austenitized for 1 h at 1050°C and tempered for 2.5 h at 780°C, a DBTT of -2.4°C and a USE of 115 J were obtained.²⁶ These values are similar to the values obtained for the 12Cr-2WV steel in the present work, even though the 12Cr-2WV steel contained 25% delta-ferrite. For other heats of 12Cr-1MoVW steel, somewhat better values were obtained.²⁶ It should be noted, however, that heat-treatment variations for the Cr-W steels could also lead to an improvement of the properties of these steels.

Investigators have concluded that small amounts of delta-ferrite^{27,28} and such ferrite accompanied by carbides at the ferrite-martensite boundaries²⁸ cause an increase in the DBTT and a decrease in the USE in 12Cr-1MoVW steel. An increase in the DBTT of about 25°C was observed for 1% delta-ferrite²⁷ and an increase of 30 to 50°C was observed when about 5% delta-ferrite was present in the microstructure.²⁸ Although the impact properties of the 12Cr-2WV steel containing 25% delta-ferrite were not as good as those of the 5Cr and 9Cr steels that were entirely martensitic (Fig. 32), they were superior to the Cr-Mo steels similarly heat treated (Fig. 33). When the results for the 12Cr-2WV steel are compared with those for the 12Cr-1MoVW, the indication is that it must be more than the delta-ferrite in the 12Cr-1MoVW steel that causes the deterioration in properties of 12Cr-1MoVW steel.^{27,28} This conclusion is supported by

impact data on 9Cr-2MoVNb that contained about 20% delta-ferrite.^{29,30} This steel also had superior properties to those of 12Cr-1MoVW steel. These results indicate that the inferior properties of the 12Cr-1MoVW steel are not caused by the delta-ferrite but may be due to the higher-carbon content (the 12 Cr-1MoVW steel contains 0.2% C against ~0.1% C for the 12Cr-2WV steel), which is known to affect impact properties.³¹ The higher carbon content leads to larger amounts of precipitate,¹¹ which could degrade the impact properties.²⁸

From these results, it appears that the use of a duplex structure of martensite and delta-ferrite should not be ruled out on the basis of impact properties. However, the 12Cr-2WV steel must be ruled out at present because its strength was not as good as the strength of the 9Cr steels and the 2.25Cr-2WV steel.

Although these steels are still at an early stage of development, the impact properties of the 2.25Cr-2WV steel were somewhat disappointing, in view of the excellent tensile properties of this steel. A mixed structure of tempered bainite and polygonal ferrite (the microstructure of the 2.25Cr-2WV) is known to have an inferior impact behavior compared to a steel with a microstructure made up of a single constituent.³² This may explain why the 2.25Cr-2W steel had the best impact behavior of the 2.25Cr steels (Table 6 and Fig. 32).

The observation that the impact behavior of a 100% bainitic steel is superior to one containing polygonal ferrite means that it should be possible to improve the impact properties of the 2.25Cr-2WV steel by heat treatment and by increasing the hardenability. By proper alloying, the hardenability of the steel can be increased and the ferrite eliminated. Finally, the type of bainite that forms can also affect the impact properties;³³ the type of bainite, in turn, depends on the hardenability.

SUMMARY AND CONCLUSIONS

By eliminating Mo, Nb, N, Ni, and Cu from steels used for fusion reactor structural components, induced radioactivity levels will more

rapidly decay to lower levels, which will allow simpler radioactive waste-disposal techniques for these reactor components when they are discarded after service. Such FIRD austenitic and ferritic steels (sometimes referred to as low-activation or reduced-activation steels) are being developed, and, in this report, preliminary work on developing ferritic steels was presented. Developmental steels were patterned on the conventional ferritic steels being considered as candidates for fusion-reactor applications--2.25Cr-1Mo, 9Cr-1MoVNb, and 12Cr-1MoVW steels. Tungsten was used as a replacement for molybdenum, and tantalum was substituted for niobium. Microstructures were examined, tempering behavior was determined, and tensile and impact tests were conducted on experimental steels in the normalized-and-tempered condition.

To determine the effect of Cr, W, V, and Ta, eight heats of steel were obtained. Alloys containing 2% W (an atom-for-atom replacement of molybdenum in the Cr-Mo steels) and 0.25% V were produced for chromium levels of 2.25, 5, 9, and 12% (designated 2.25Cr-2WV, 5Cr-2WV, 9Cr-2WV, and 12Cr-2WV). A 9Cr-2WV steel with 0.07% Ta (9Cr-2WVTa) was also produced, along with 2.25Cr steels with 0.25% V and 0 and 1% W (2.25CrV, and 2.25Cr-1WV) and with 2% W and no vanadium (2.25Cr-2W). Carbon was maintained at 0.1% for all of the steels.

Optical microstructures of the normalized-and-tempered steels showed an effect of tungsten on hardenability. The 2.25CrV and 2.25Cr-1WV contained 70% and 45% polygonal ferrite, respectively, the balance bainite, while the 2.25Cr-2WV steel contained 15-20% ferrite, the balance bainite. The 2.25Cr-2W steel was 100% bainite. The 5Cr and 9Cr steels were entirely martensitic, but the 12Cr-2WV steel contained approximately 25% delta-ferrite. Additions of manganese and/or carbon to the base 12Cr-2WV would be needed to eliminate the delta ferrite. A combination of 0.2% C and 1.5% Mn should yield a fully martensitic structure.

Hardness measurements as a function of different tempering treatments indicated that the tempering resistance of the 2.25Cr-2WV, 5Cr-2WV, 9Cr-2WV, and 12Cr-2WV were similar for long tempering times and/or high tempering temperatures. These steels had tempering resistances similar to those for the 9Cr-1MoVNb and 12Cr-1MoVW steels.

Tensile studies indicated that an atom-for-atom replacement of molybdenum by tungsten resulted in a steel with properties similar to those of the analogous Cr-Mo steel, when both were heat treated similarly. The properties of the 2.25Cr-2W steel were similar to those of 2.25Cr-1Mo steel. Likewise, the properties of 9Cr-2WVTa steel were similar to those for the 9Cr-1MoVNb, indicating that tantalum could replace niobium. Tensile properties for the 12Cr-2WV were inferior to those of the 12Cr-1MoVW steel, because of the large amount of delta-ferrite in the Cr-W steel. Of the eight experimental steels, the 2.25Cr-2WV and the 9Cr-2WVTa steels were the strongest. Both had properties similar to the strongest Cr-Mo steels, when all steels were heat treated similarly.

Impact properties of the 5Cr-2WV, 9Cr-2WV, 9Cr-2WVTa, and 12Cr-2WV steels were superior to those for 9Cr-1MoVNb and 12Cr-1MoVW steels, when all steels were given similar heat treatments. The excellent impact properties of the 12Cr-2WV steel occurred despite the 25% delta-ferrite in the microstructure. Impact properties of the 2.25Cr-2WV steel, which had excellent tensile properties relative to the other Cr-W steels, were inferior to those of the high-chromium (5-12% Cr) steels. This difference was attributed to microstructure, and the development of a low-chromium FIRD steel with good strength and impact behavior should be possible with further alloying and proper heat treatment.

Results from these preliminary tests indicate that it should be possible to develop FIRD ferritic steels with properties similar to the ferritic steels presently being considered in the fusion program. In the future, we propose further alloying to improve on the properties of the steels presented in this report. We feel that FIRD ferritic steels can be developed with better properties than those of the Cr-Mo steels presently in the program. Furthermore, such improved steels should be possible over a range of chromium concentrations, from as low as 2.25% to as high as 12%.

ACKNOWLEDGMENTS

We wish to thank the following people who helped in the completion of this work: L. T. Gibson, N. H. Rouse, E. L. Ryan, and T. D. Owings, Jr. carried out the experimental tests and procedures; C. W. Houck did the optical metallography; J. M. Vitek and D. J. Alexander reviewed the manuscript; and G. R. Carter prepared the manuscript.

REFERENCES

1. R. W. Conn et al., *Panel Report on Low Activation Materials for Fusion Applications*, UCLA Report PPG-728, University of California at Los Angeles, June 1983.
2. Nuclear Regulatory Commission, "Licensing Requirements for Land Disposal of Radioactive Waste," 10 CFR Part 61, *Fed. Regis.* 47(248), 57446-82 (Dec. 27, 1982).
3. R. L. Klueh and E. E. Bloom, "The Development of Ferritic Steels for Fast Induced-Radioactivity Decay for Fusion Reactor Applications," *Nucl. Eng. Design/Fusion* 2, 383-9 (1985).
4. R. W. Honeycombe, *Structure and Strength of Alloy Steels*, Climax Molybdenum Company, London, 1974.
5. N. M. Ghoniem, A. Shabaik, and M. Z. Youssef, "Development of Low Activation Vanadium Steel for Fusion Applications," pp. 201-08 in *Ferritic Alloys for use in Nuclear Energy Technologies*, The Metallurgical Society of AIME, Warrendale, Pa., 1984.
6. D. S. Gelles and M. L. Hamilton, "Effects of Irradiation on Low Activation Ferritic Alloys," *J. Nucl. Mater.* 148, 272-8 (1987).
7. T. Noda, F. Abe, H. Araki, and M. Okada, "Development of Low Activation Ferritic Steels," *J. Nucl. Mater.* 141-143, 1102-06 (1986).
8. C. Y. Hsu and T. A. Lechtenberg, "Microstructure and Mechanical Properties of Unirradiated Low Activation Ferritic Steel," *J. Nucl. Mater.* 141-143, 1107-12 (1986).
9. D. Dulieu, K. W. Tupholme, and G. J. Butterworth, "Development of Low-Activation Martensitic Stainless Steels," *J. Nucl. Mater.* 141-143, 1077-101 (1986).

10. M. Tamura, H. Hayakawa, M. Tanimura, A. Hishinuma, and T. Kondo, "Development of Potential Low Activation Ferritic and Austenitic Steels," *J. Nucl. Mater.* 141-143, 1067-73 (1986).
11. J. M. Vitek and R. L. Klueh, "Precipitation Reactions During the Heat Treatment of Ferritic Steels," *Metall. Trans.* 14A, 1047-55 (1983).
12. W. C. Leslie, *The Physical Metallurgy of Steels*, McGraw-Hill Book Company, New York, 1981, p. 219.
13. R. W. K. Honeycombe, "Ferrite," *Metal Science* 14, 201-14 (1980).
14. P. R. Willyman and R. W. K. Honeycombe, "Relation Between Transformation Kinetics and Mechanical Properties of Vanadium Steels," *Met. Sci.* 16, 295-303 (1982).
15. R. G. Baker and J. Nutting, "The Tempering of 2.25%Cr-1%Mo Steel After Quenching and Normalizing," *J. Iron Steel Inst.*, London 192, 257-68 (1959).
16. B. J. Shaw, "A Study of Carbides Formed in Low-Alloy Chrome-Moly Steels," pp. 117-128 in *Research on Chrome-Moly Steel*, R. S. Swift, ed., MPC-21, American Society of Mechanical Engineers, New York, 1984.
17. J. M. Vitek, ORNL, unpublished research, 1984.
18. P. J. Maziasz, R. L. Klueh, and J. M. Vitek, "Helium Effects on the Void Formation in 9 Cr-1MoVNb and 12 Cr-1MoVW Irradiated in HFIR," *J. Nucl. Mater.* 141-143, 929-37 (1986).
19. N. Igata, "Ferritic/Martensitic Dual-Phase Steel as Fusion Reactor Materials," *J. Nucl. Mater.* 133&134, 141-8 (1985).
20. Babcock and Wilcox Company, *Intermediate Croloy Steels*, Babcock and Wilcox Company, Tubular Products Division, Beaver Falls, Pa., 1971.
21. J. Orr, F. R. Beckitt, and G. D. Fawkes, "The Physical Metallurgy of Chromium-Molybdenum Steels for Fast Reactor Boilers," pp. 91-109 in *Ferritic Steels for Fast Reactor Steam Generators*, British Nuclear Energy Society, London, 1978.
22. M. K. Booker, V. K. Sikka, and B. L. P. Booker, "Comparison of Mechanical Strength Properties of Several High-Chromium Ferritic Steels," pp. 257-253 in *Ferritic Steels for High-Temperature Applications*, American Society for Metals, Metals Park, Ohio, 1983.
23. R. L. Klueh, "Chromium-Molybdenum Steels for Fusion Reactor First Walls—A Review," *Nucl. Eng. Design/Fusion* 72, 329-44 (1982).

24. F. A. Smidt, Jr., J. R. Hawthorne, and V. Provenzano, "Fracture Resistance of HT-9 After Irradiation at Elevated Temperature," pp. 269-74 in *Effects of Radiation Materials*, ASTM STP 725, D. Kramer, H. R. Brager, and J. S. Perrin, eds., American Society for Testing and Materials, Philadelphia, 1981.

25. J. M. Vitek, W. R. Corwin, R. L. Klueh, and J. R. Hawthorne, "On the Saturation of the DBTT Shift of Irradiated 12Cr-1MoVW With Increasing Fluence," *J. Nucl. Mater.* 141-143, 948-53 (1986).

26. W. R. Corwin and A. M. Hougland, "Effect of Specimen Size and Material Condition on the Charpy Impact Properties of 9Cr-1Mo-V-Nb Steel," pp. 325-38 in *The Use of Small Scale Specimens for Testing Irradiated Material*, ASTM STP 888, W. R. Corwin and G. E. Lucas, eds., American Society for Testing and Materials, Philadelphia, 1986.

27. K. Anderko, K. David, W. Ohly, M. Schirra, and C. Wassilew, "Optimization Work on Niobium Stabilized 12% CrMoVNb Martensitic Steels for Breeder and Fusion Reactor Applications," pp. 299-306 in *Ferritic Alloys for Use in Nuclear Energy Technologies*, The Metallurgical Society of AIME, Warrendale, Pa., 1984.

28. B. A. Chin and R. C. Wilcox, "The Effect of Heat Treatment on the Impact Properties of a 12Cr-1Mo-V-W Steel," pp. 347-56 in *Ferritic Alloys for use in Nuclear Energy Technologies*, The Metallurgical Society of AIME, Warrendale, Pa., 1984.

29. Y. Hosoi, N. Wade, T. Urita, M. Tannino, and H. Komatsu, "Change in Microstructure and Toughness of Ferritic-Martensitic Stainless Steels During Long-Term Aging," *J. Nucl. Mater.* 133&134, 337-42 (1984).

30. Y. Hosoi, N. Wade, S. Kunitatsu, and T. Urita, "Precipitation Behavior of Laves Phase and Its Effect on Toughness of 9Cr-2Mo Ferritic-Martensitic Steel," *J. Nucl. Mater.* 141-143, 461-5 (1986).

31. F. B. Pickering, *Physical Metallurgy and the Design of Steels*, Applied Science Publishers, Ltd., London, 1978.

32. D. A. Canonico, Combustion Engineering, Chattanooga, Tenn., private communication, 1987.

33. R. L. Klueh, "Bainite in Cr-Mo Steels," pp. 601-06 in *Martensitic Transformations (COMAT)*, Japan Institute of Metals, Sendai, Japan, 1987.

ORNL-6472
 Distribution
 Category UC-423

INTERNAL DISTRIBUTION

1-2. Central Research Library	31-35. P. J. Maziasz
3. Document Reference Section	36. M. K. Miller
4-5. Laboratory Records Department	37. R. K. Nanstad
6. Laboratory Records, ORNL RC	38. S. J. Pawel
7. ORNL Patent Section	39. P. L. Rittenhouse
8. D. J. Alexander	40. A. F. Rowcliffe
9. J. Bentley	41. V. K. Sikka
10. E. E. Bloom	42. G. M. Slaughter
11. K. W. Boling	43. J. O. Stiegler
12. C. R. Brinkman	44. R. W. Swindeman
13-17. W. R. Corwin	45-47. P. T. Thornton
18. D. F. Craig	48. P. F. Tortorelli
19. G. M. Goodwin	49. J. M. Vitek
20. M. L. Grossbeck	50. F. W. Wiffen
21. F. M. Haggag	51. H. D. Brody (Consultant)
22. R. L. Heestand	52. G. Y. Chin (Consultant)
23. J. R. Keiser	53. F. F. Lange (Consultant)
24. O. F. Kimball	54. W. D. Nix (Consultant)
25. J. F. King	55. D. P. Pope (Consultant)
26-30. R. L. Klueh	56. E. R. Thompson (Consultant)

EXTERNAL DISTRIBUTION

57-59. BATTELLE-PACIFIC NORTHWEST LABORATORY, P.O. Box 999, Richland, WA 99352

F. A. Garner
 D. G. Gelles
 M. L. Hamilton

60. CARNEGIE INSTITUTE OF TECHNOLOGY, Carnegie-Mellon University, Schenley Park, Pittsburgh, PA 15213

W. M. Garrison, Jr.

61. GA TECHNOLOGIES, INC., P.O. Box 85608, San Diego, CA 92138

T. A. Lechtenberg

62. MCDONNELL-DOUGLAS ASTRONAUTICS COMPANY, East, P.O. Box 516, Bldg. 92, St. Louis, MO 63166

J. W. Davis

63. RENSSELAER POLYTECHNIC INSTITUTE, Troy, NY 12181

D. Steiner

64. UNIVERSITY OF CALIFORNIA, Department of Chemical and Nuclear
Engineering, Santa Barbara, CA 93106

G. R. Lucas

65-67. UNIVERSITY OF CALIFORNIA, Department of Chemical, Nuclear and
Thermal Engineering, Los Angeles, CA 90024

M. A. Abdou

R. W. Conn

N. M. Ghoniem

68-71. DEPARTMENT OF ENERGY, Office of Fusion Energy, Washington,
DC 20545

S. E. Berk

J. F. Clarke

M. M. Cohen

T. C. Reuther

72. DOE, OAK RIDGE OPERATIONS OFFICE, P.O. Box 2001, Oak Ridge,
TN 37831

Assistant Manager for Energy Research and Development

73-120. DOE, OFFICE OF SCIENTIFIC AND TECHNICAL INFORMATION, P.O. Box 62,
Oak Ridge, TN 37831

For distribution as shown in DOE/TIC-4500, Distribution
Category UC-423 (Magnetic Fusion Reactor Materials).